AE 658

Aerodynamic Design of Intakes and Propelling Nozzles

Intakes

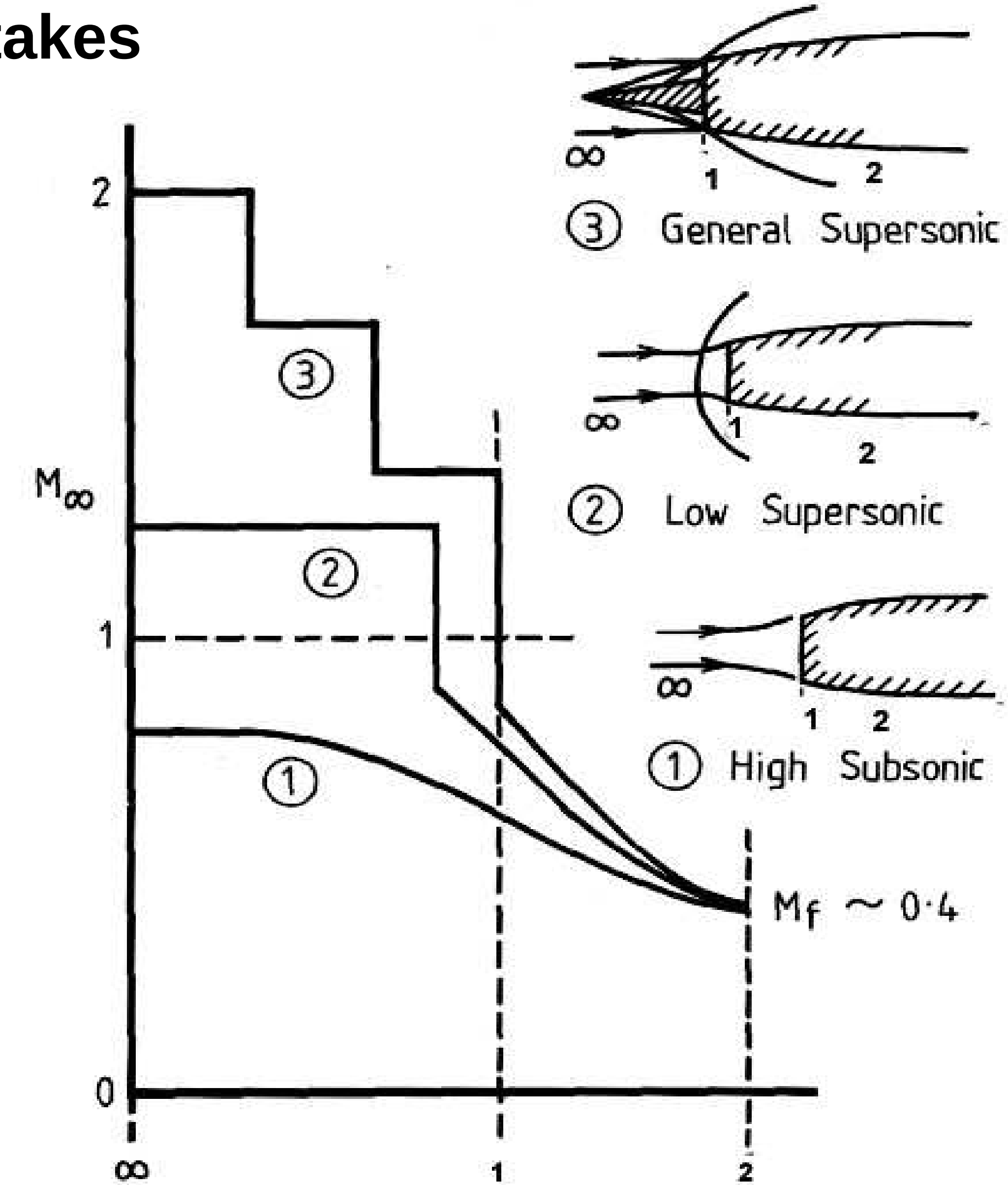

flow retardation for subsonic, transonic and supersonic intakes.

Subsonic Intakes

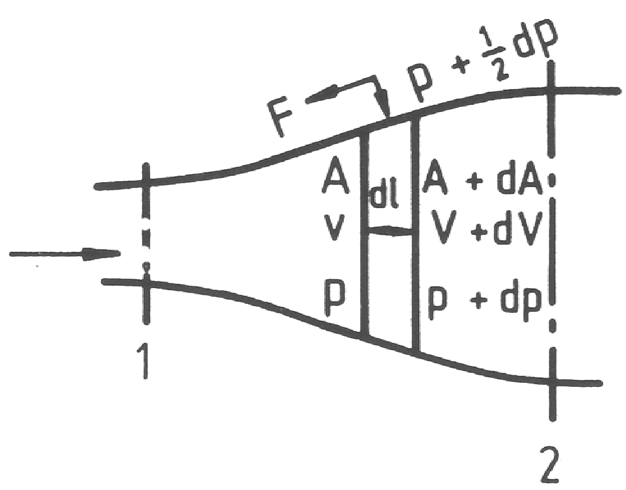

Streamtube with boundary

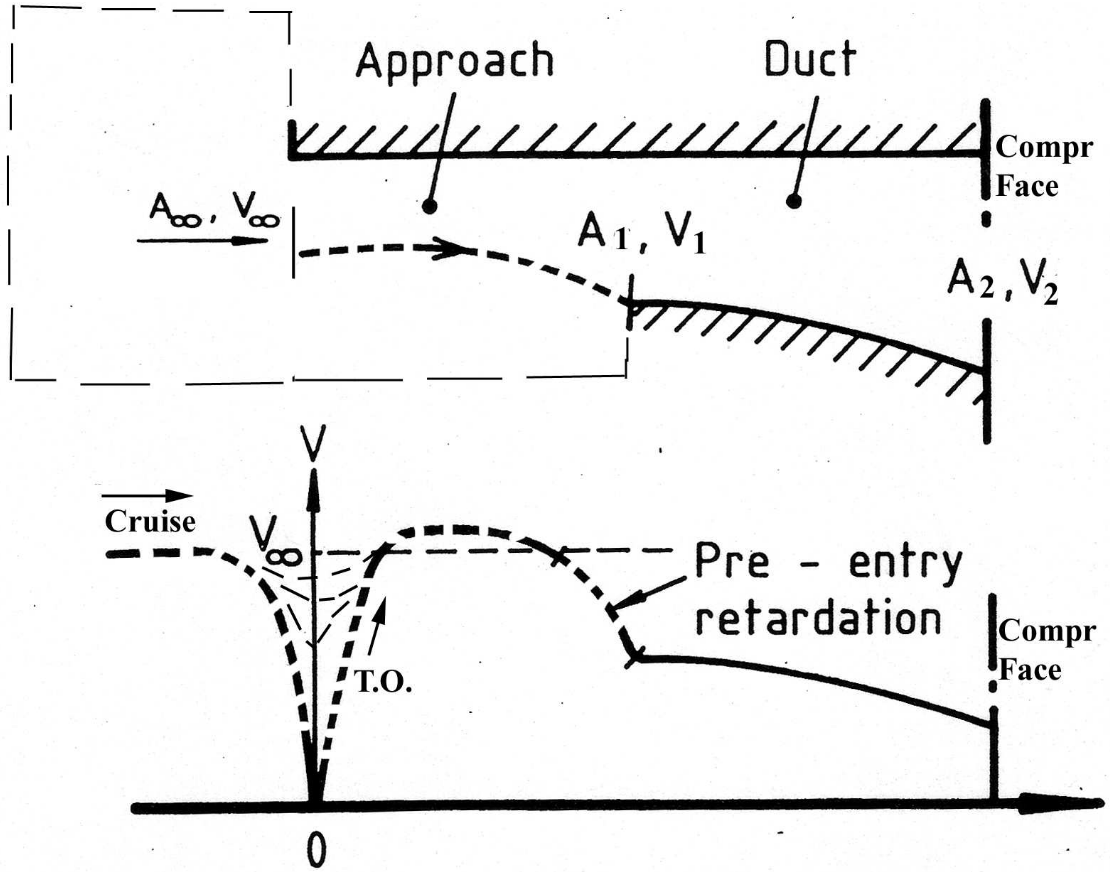

Representation of internal flow with external wetted surface.

Subsonic Intakes

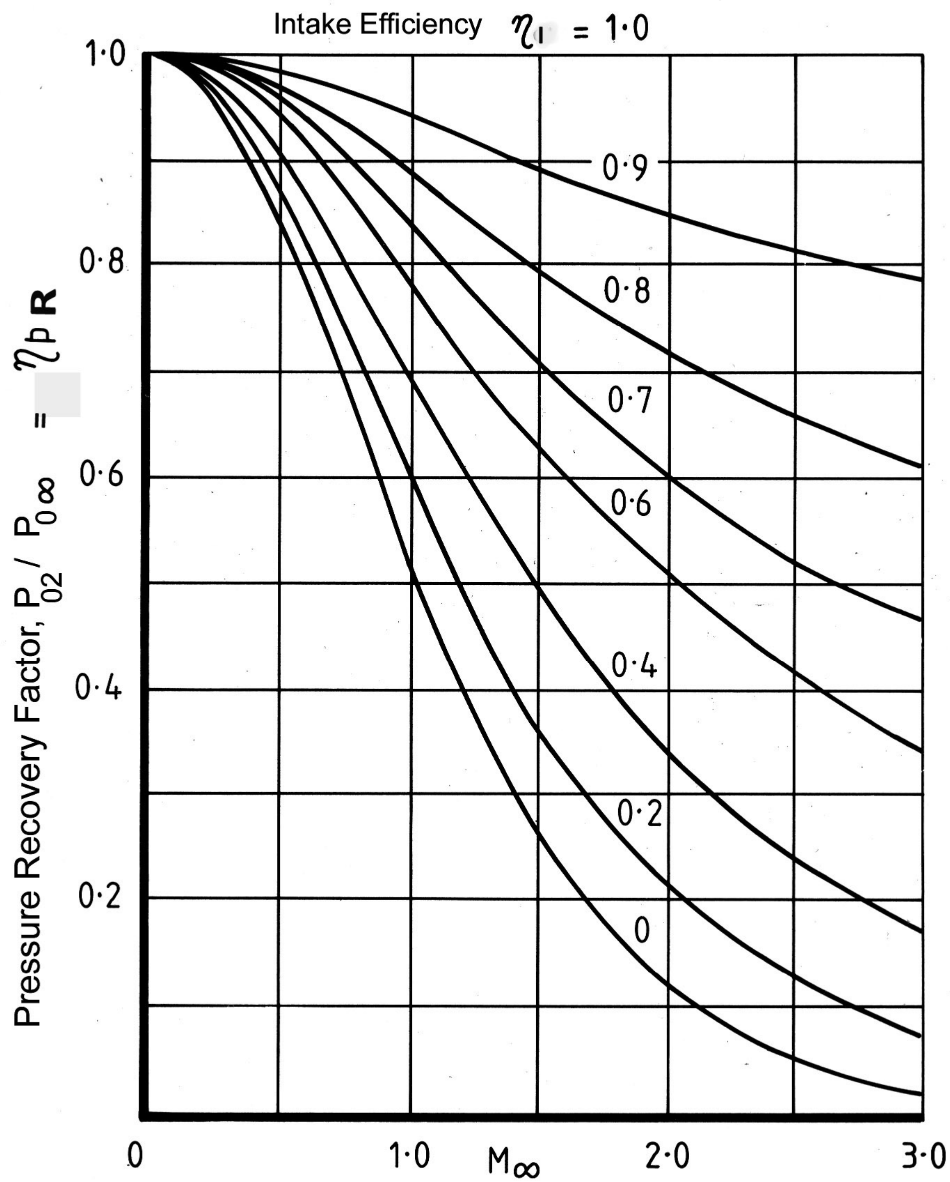

Relationship between η_I and η_{PR}

Subsonic Intakes

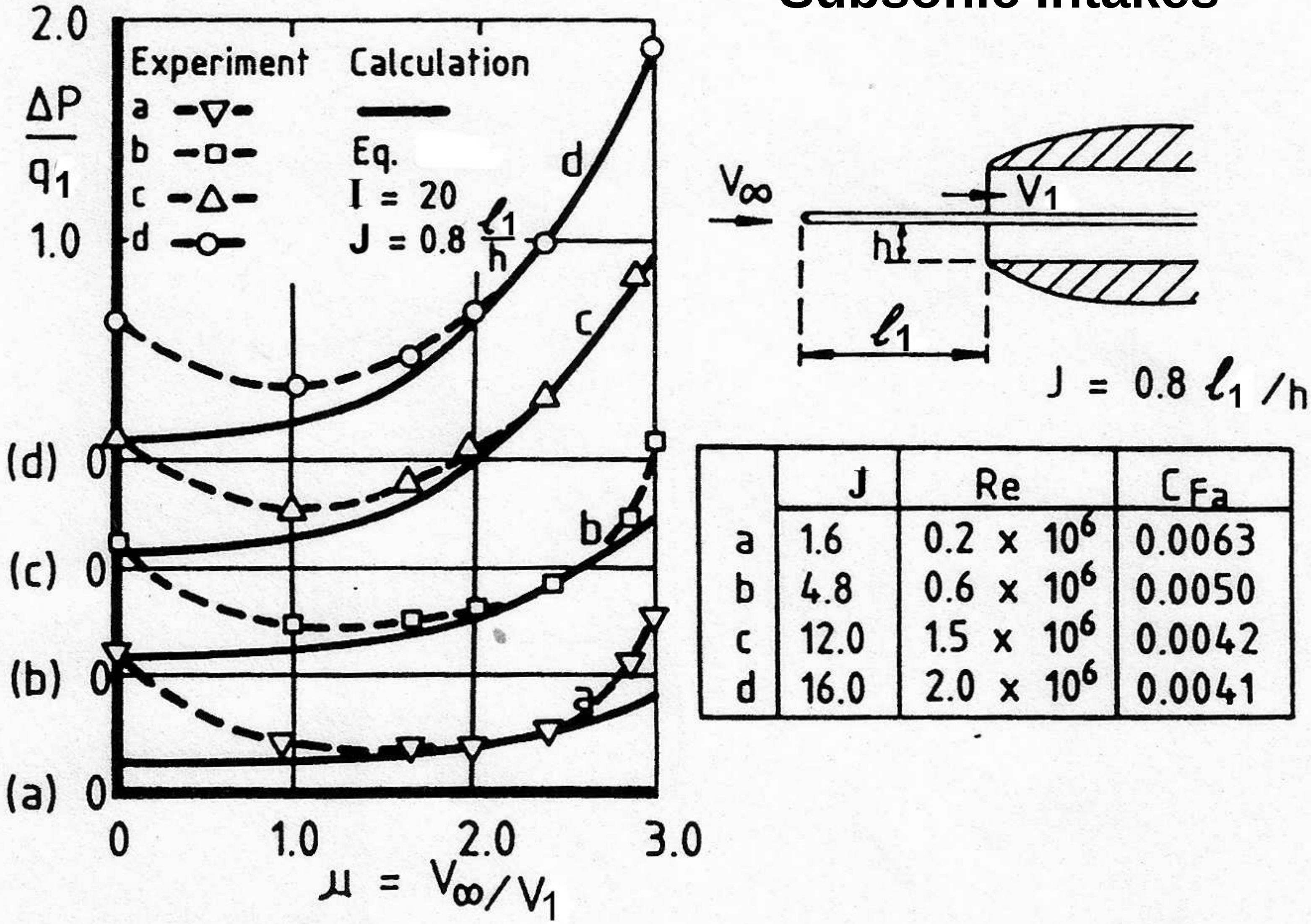

	J	Re	C_{Fa}
a	1.6	0.2×10^6	0.0063
b	4.8	0.6×10^6	0.0050
c	12.0	1.5×10^6	0.0042
d	16.0	2.0×10^6	0.0041

Comparison of Equation with experimental results

Subsonic Intakes

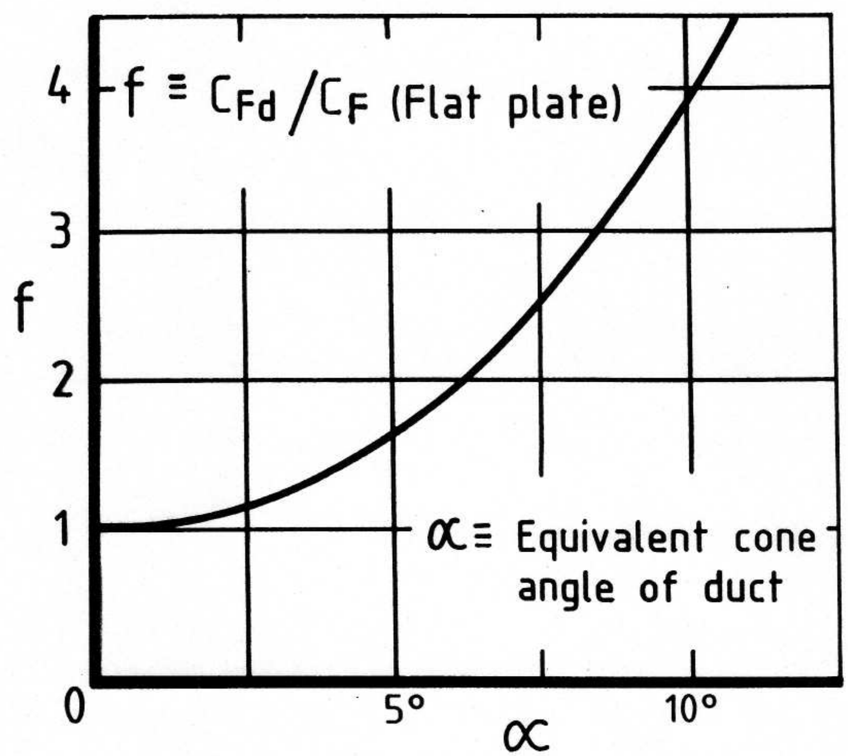

Effective friction coefficient in duct deduced from experiments

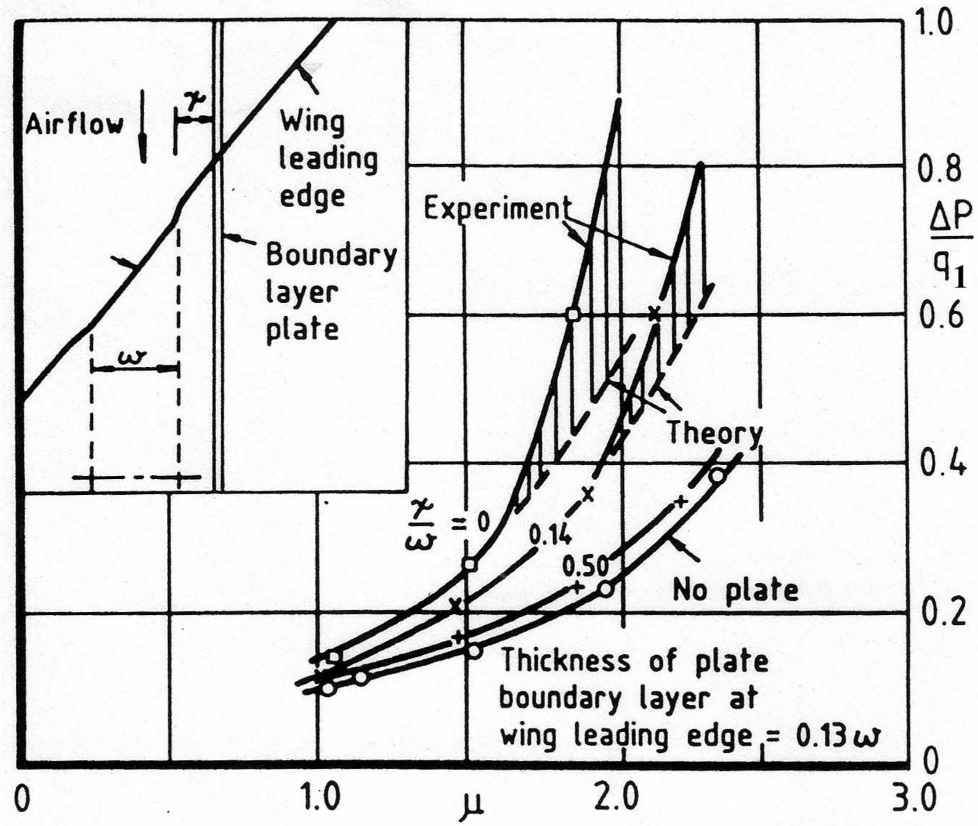

Intakes: pre-entry flow separation.

Subsonic Intakes

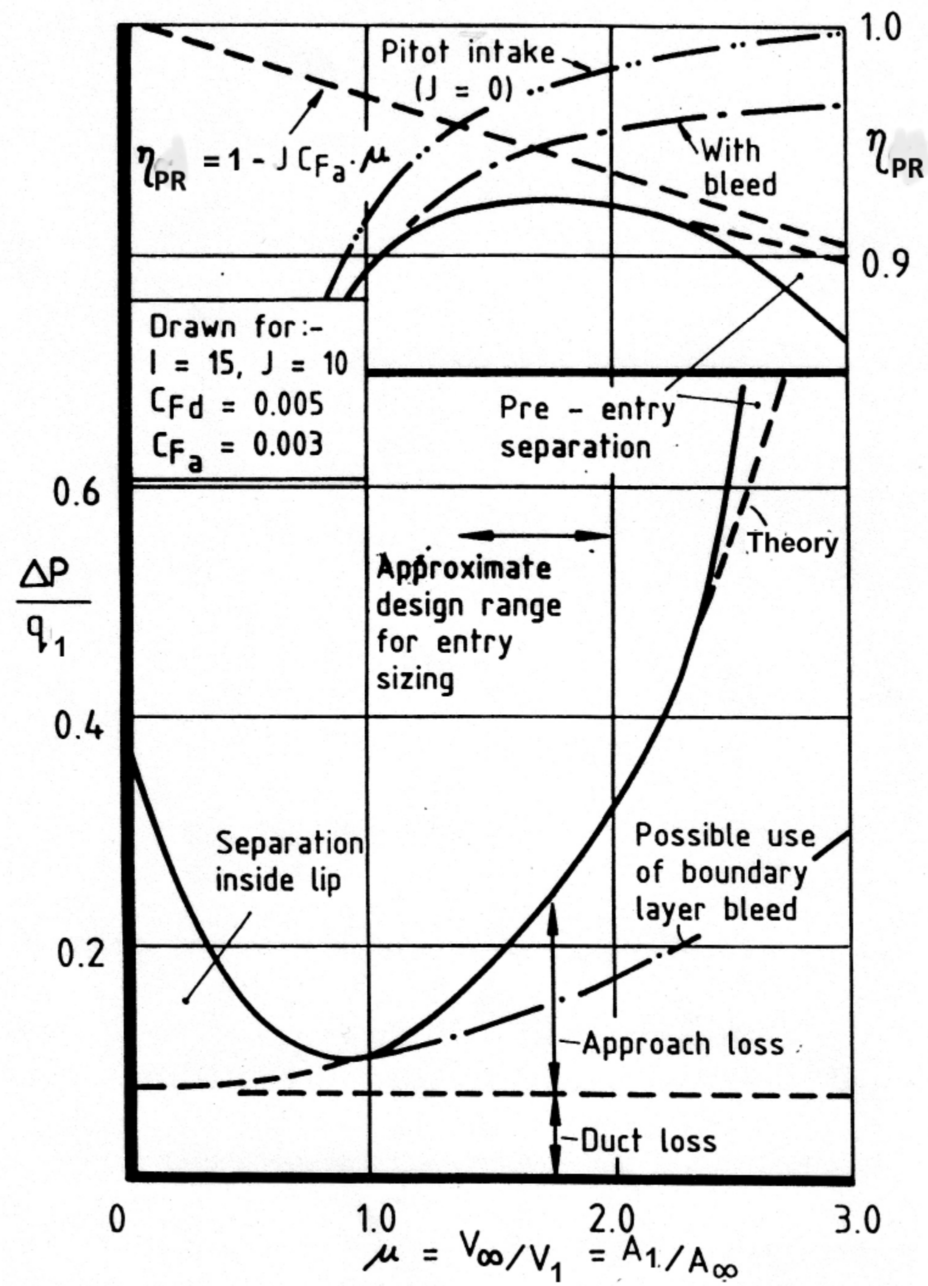

Loss and Recovery Chararcteristics of subsonic Intakes

Subsonic Intakes

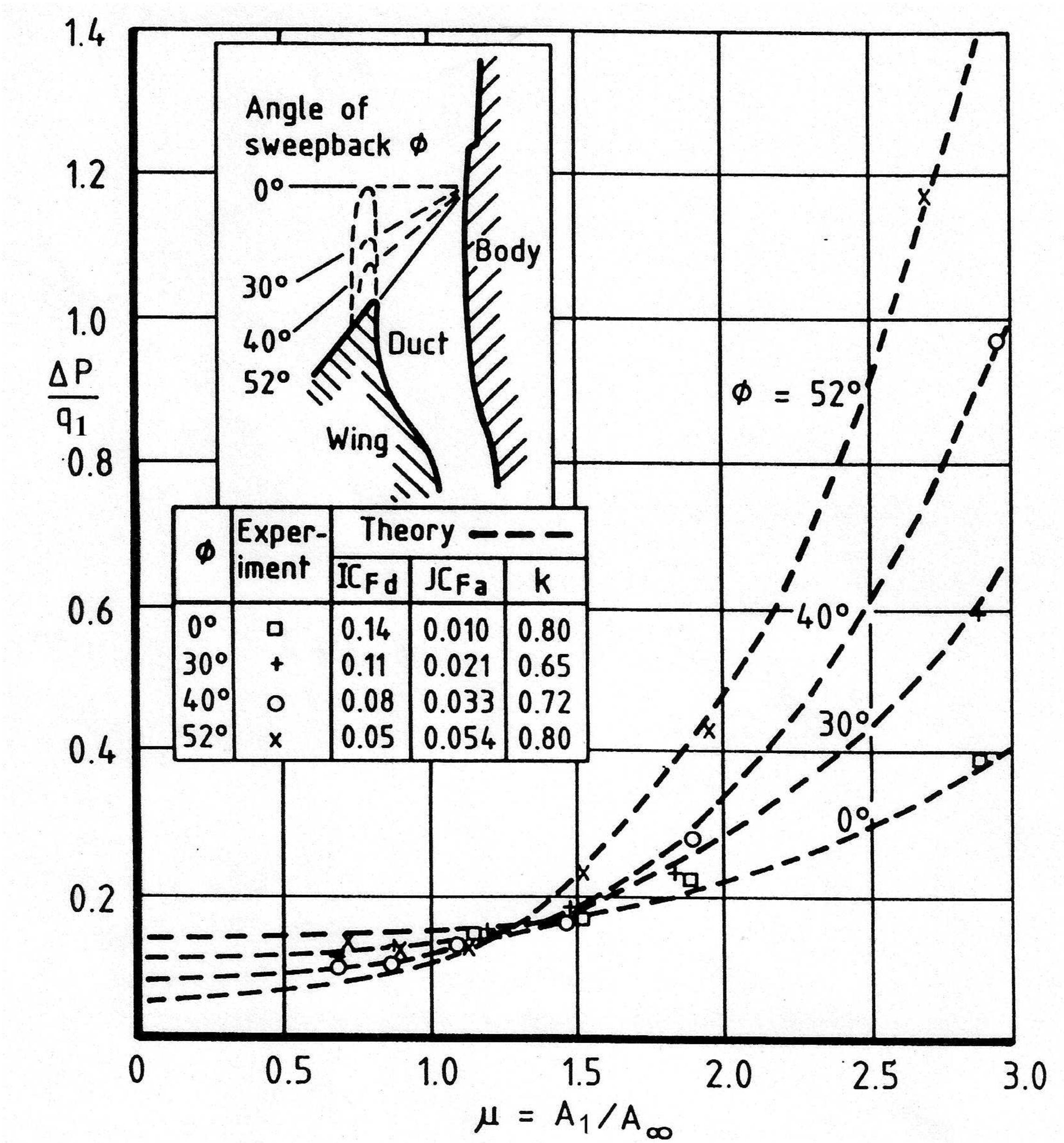

Loss in leading-edge intakes at various angles of sweep.

Subsonic Intakes

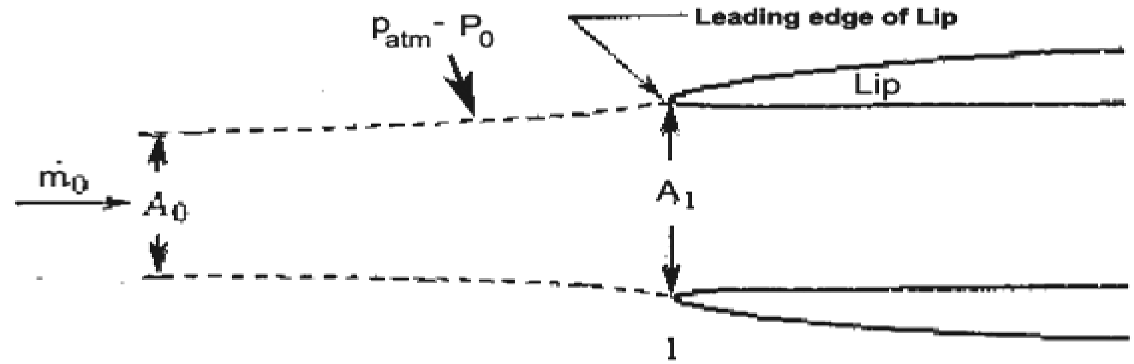

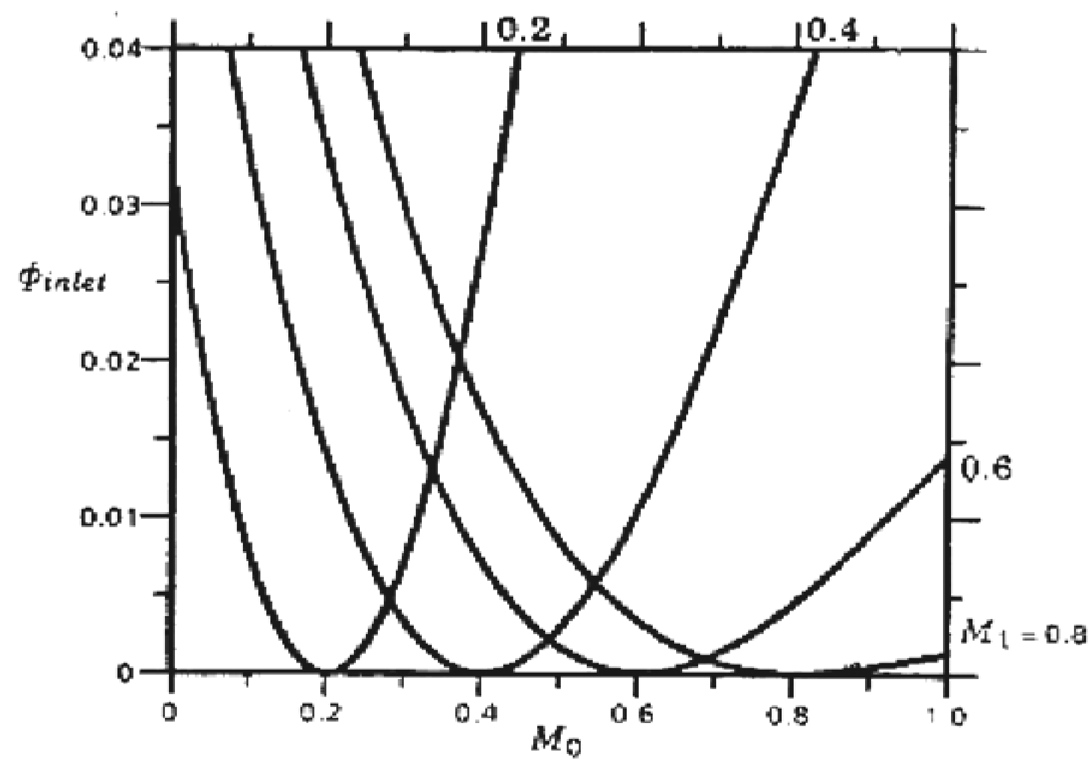

Subsonic Intakes

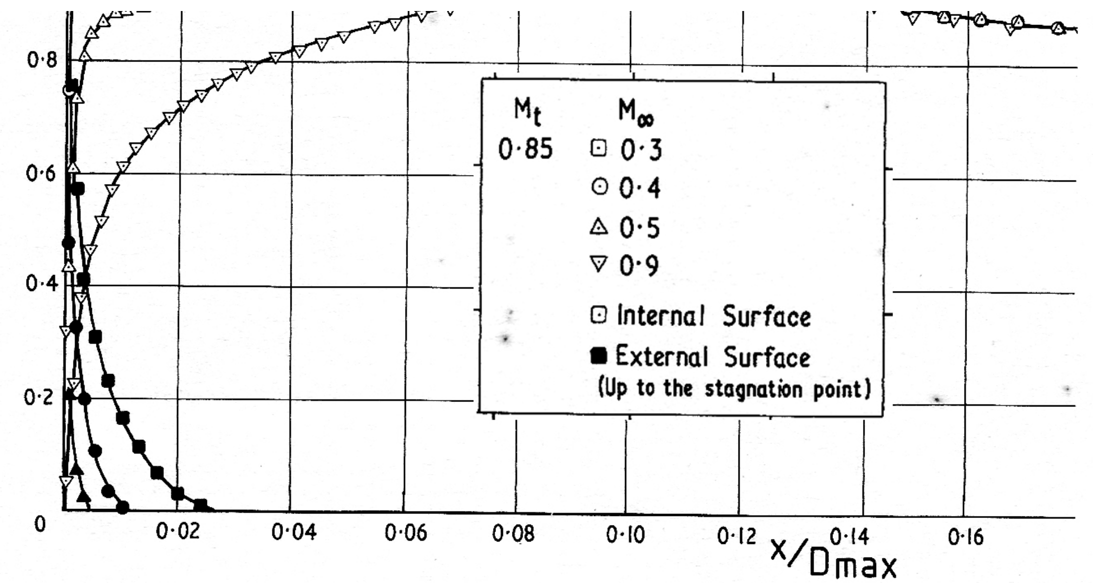

Effect of forward speed on lip surface Mach number distribution (ellipse ratio a/b 5, contraction ratio 1.15).

Subsonic Intakes

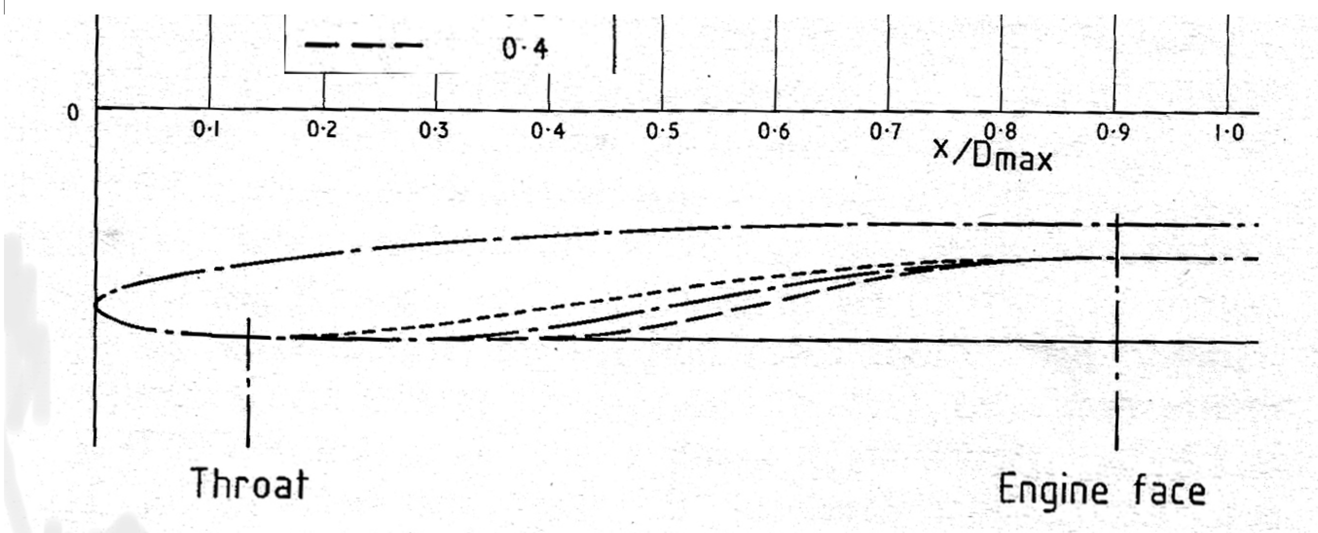

Influence of duct shape on lip and duct surface Mach number distributions.

Subsonic Intakes

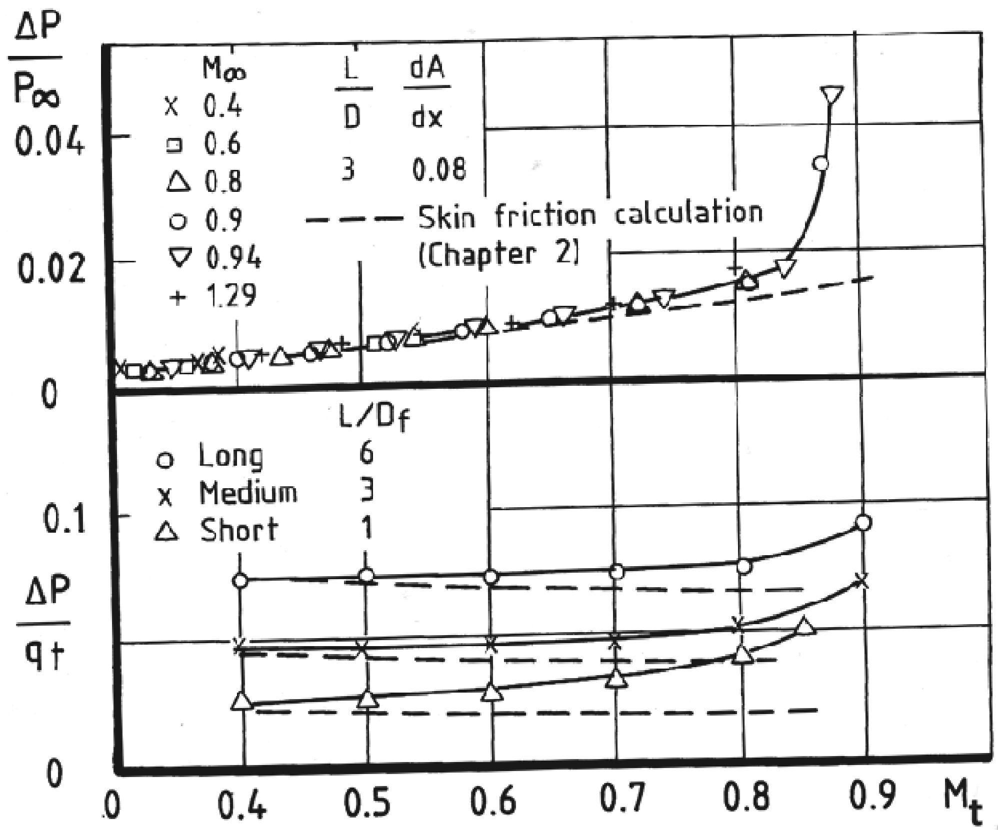

Duct total-pressure loss.

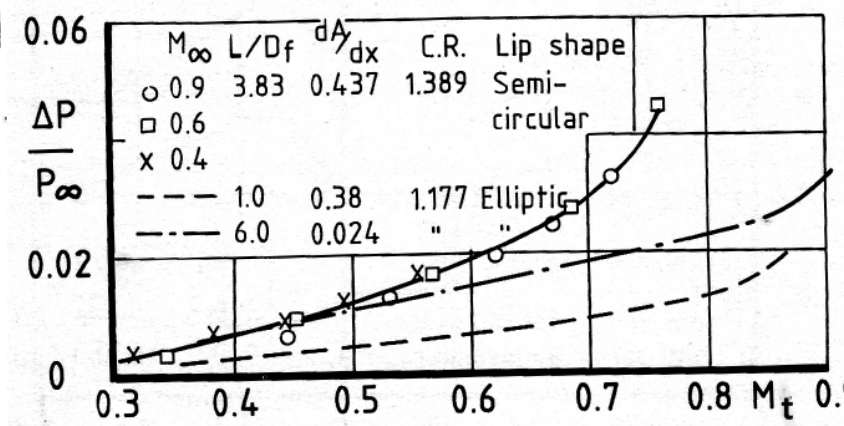

Influence of lip shape on duct total-pressure loss.

Subsonic Intakes

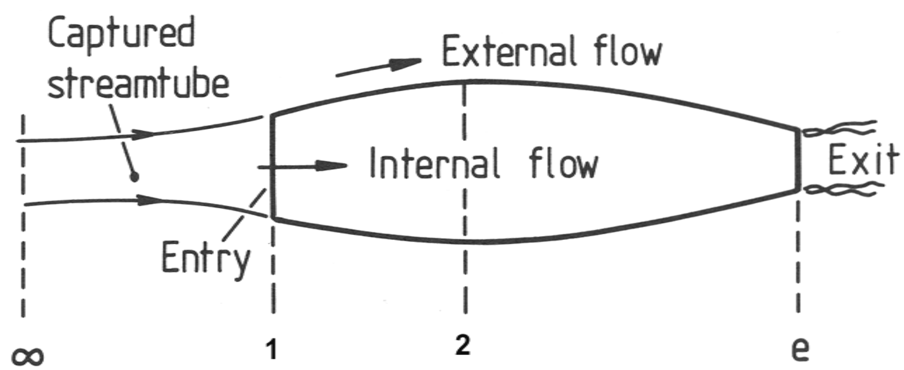

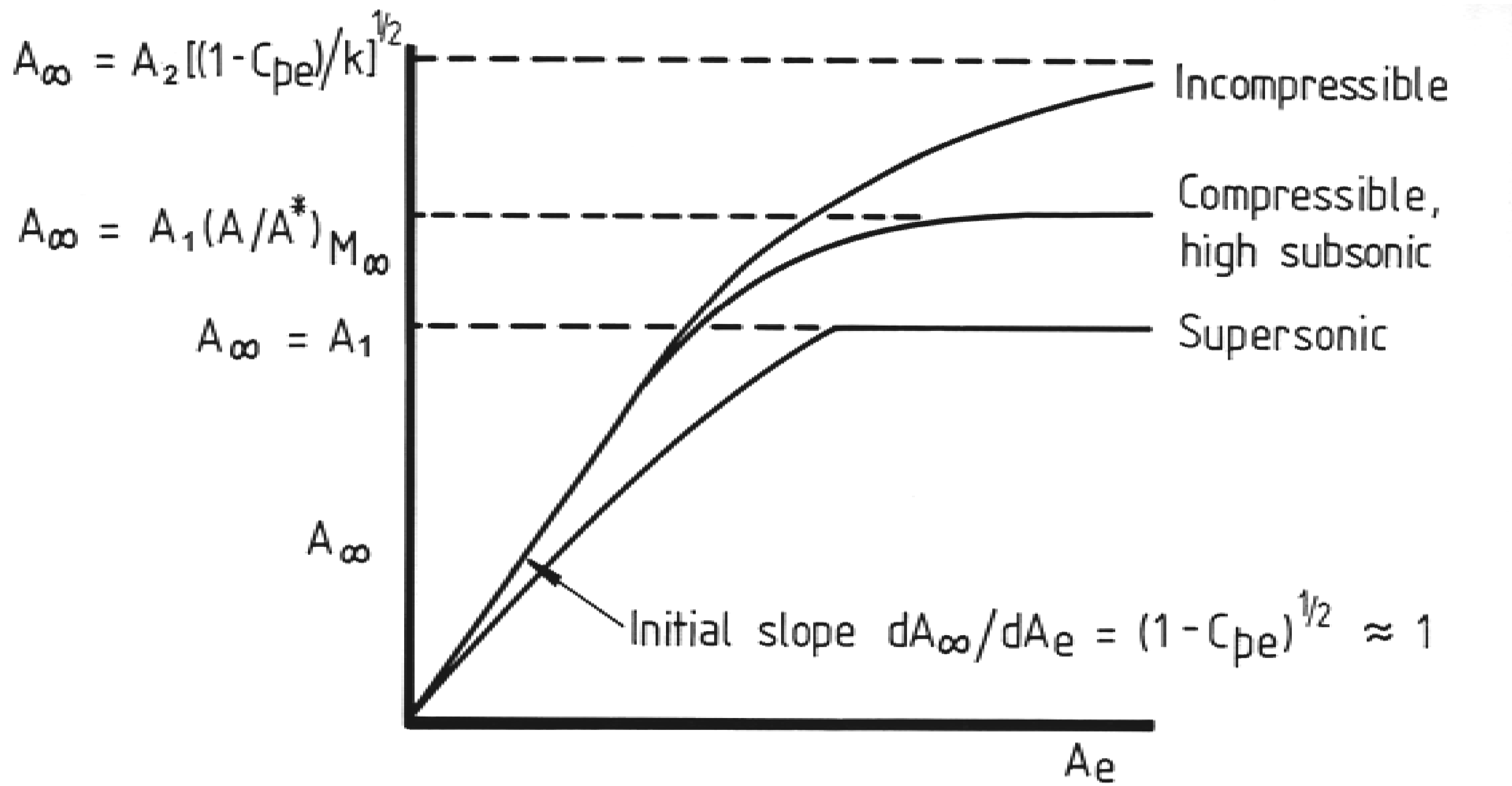

Types of variation of capture area with exit area.

Subsonic Intakes

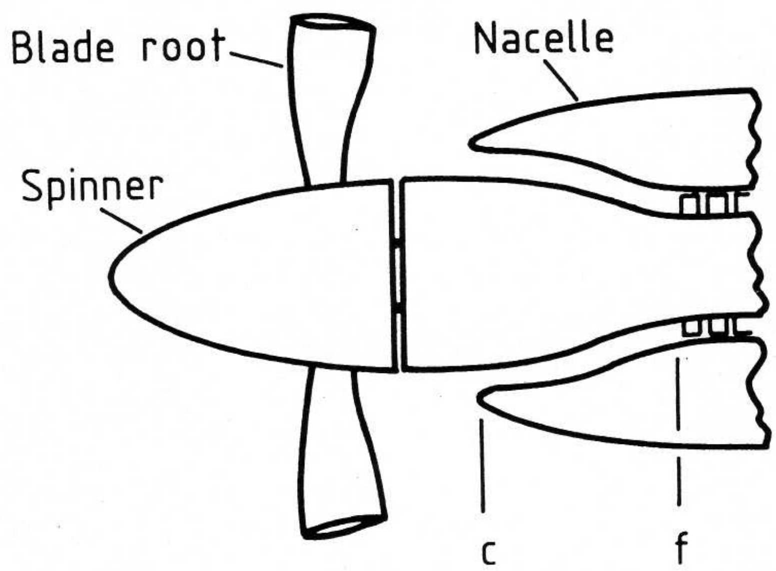

Propeller intake.

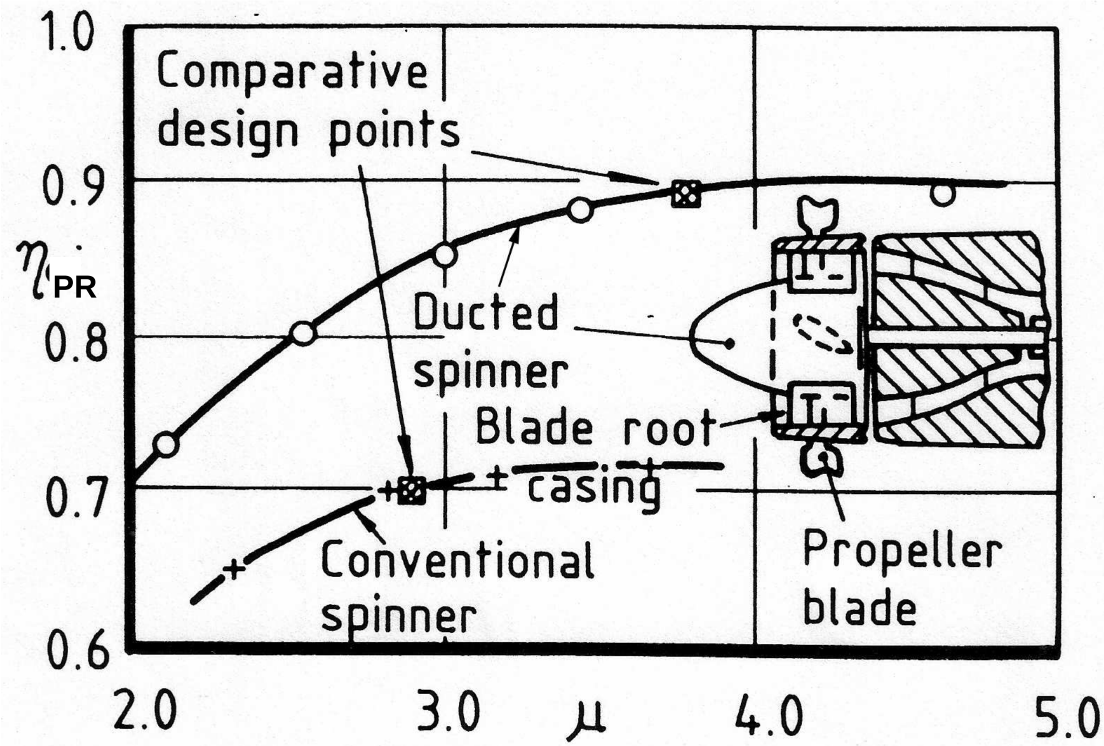

Ducted spinner for propeller intake.

Transonic Intakes

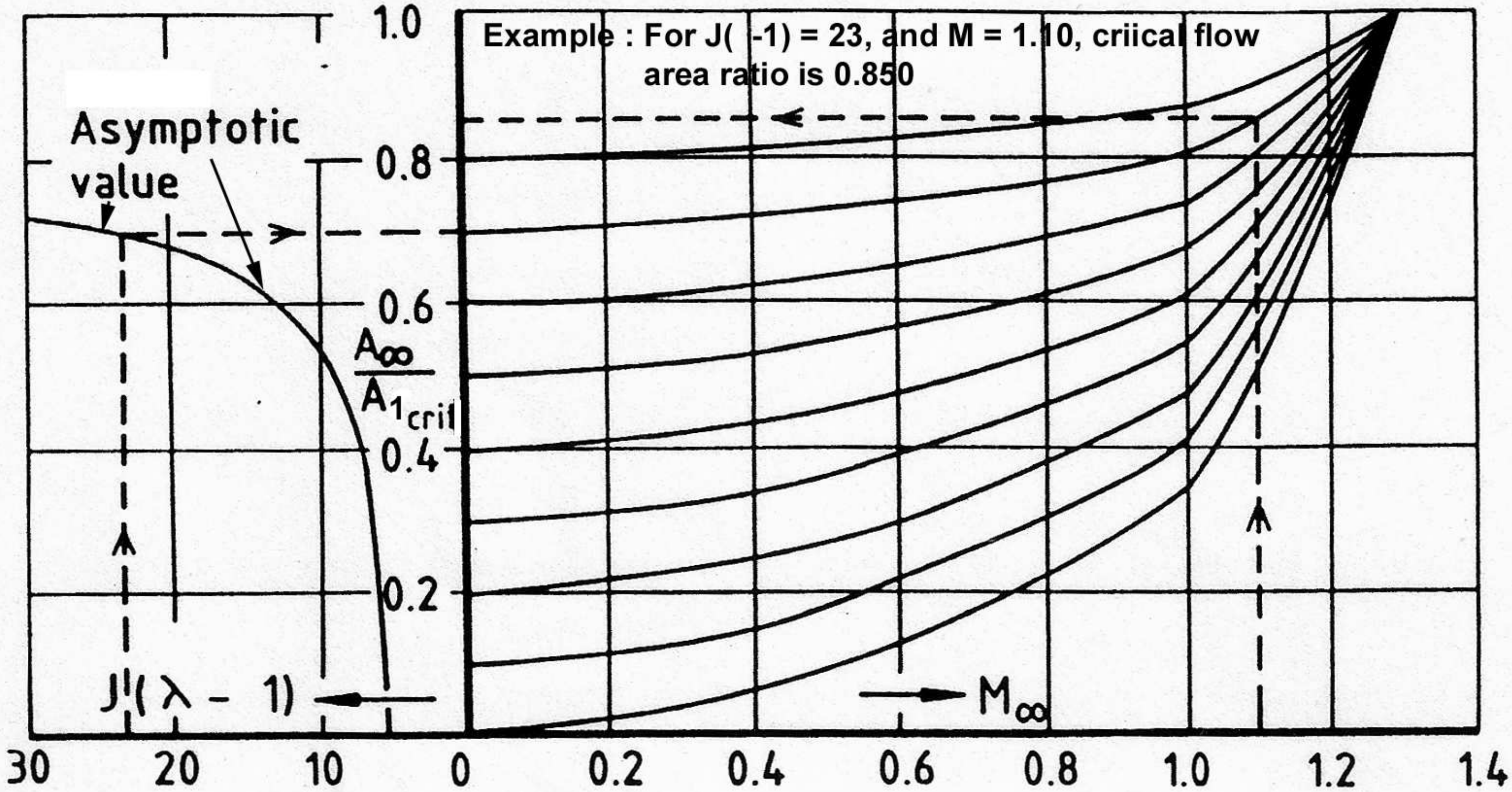

Critical flow ratio for pre-entry separation.

[$\lambda =$ Total perimeter of the intake mouth / characteristic diameter]

Transonic Intakes

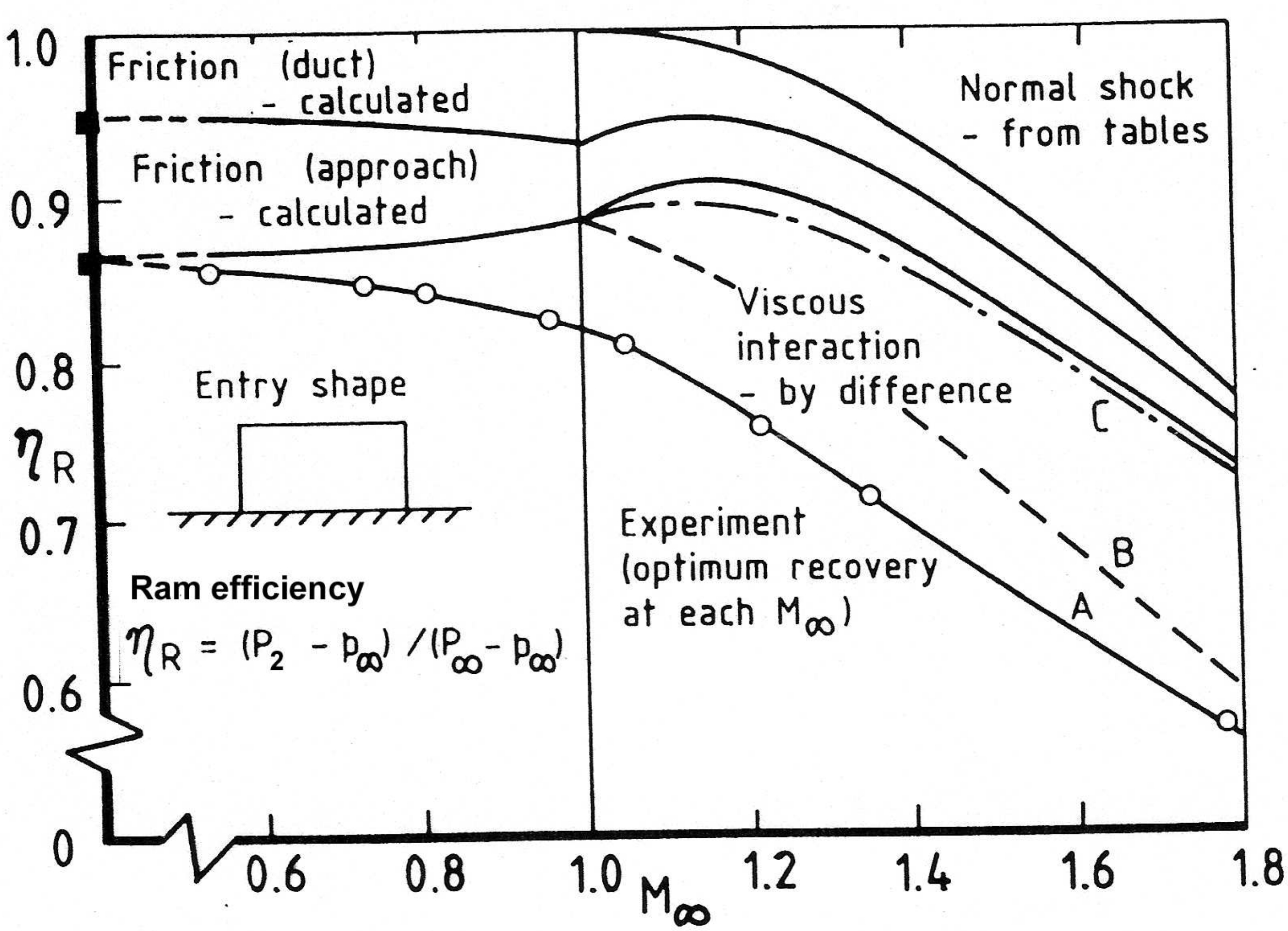

Breakdown of loss at subsonic and supersonic speeds.

Supersonic Intakes

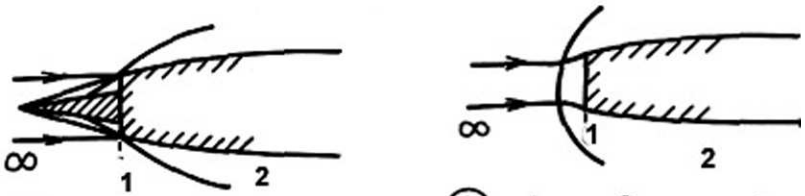

(1) General Supersonic (2) Low Supersonic

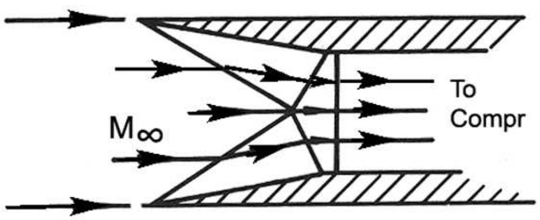

(a)

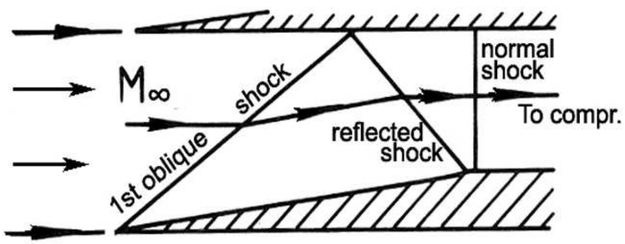

(b)

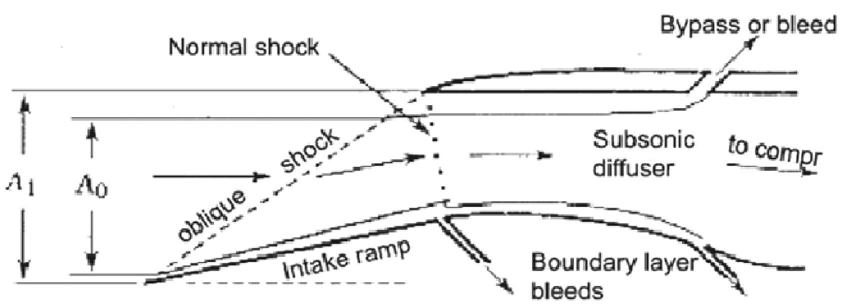

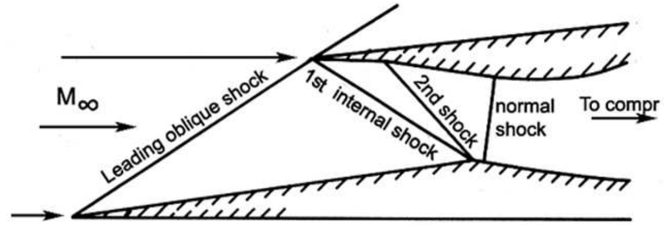

(c)

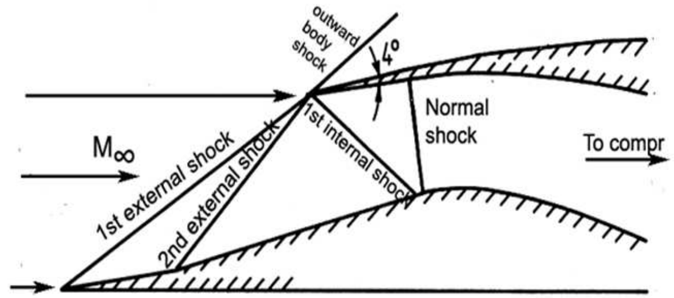

(d)

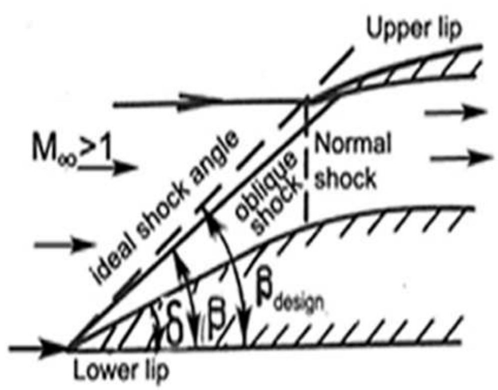

(a) $\beta \leq \beta_{optimum}$

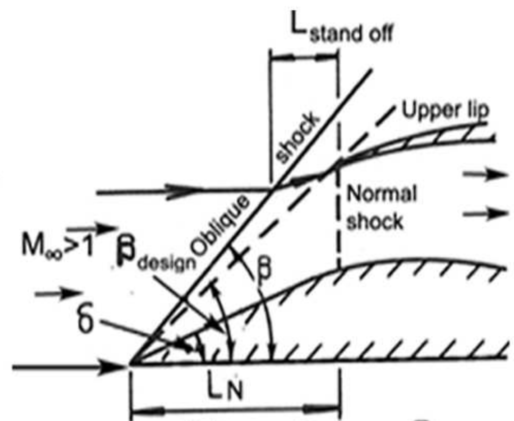

(b) $\beta > \beta_{opt}$

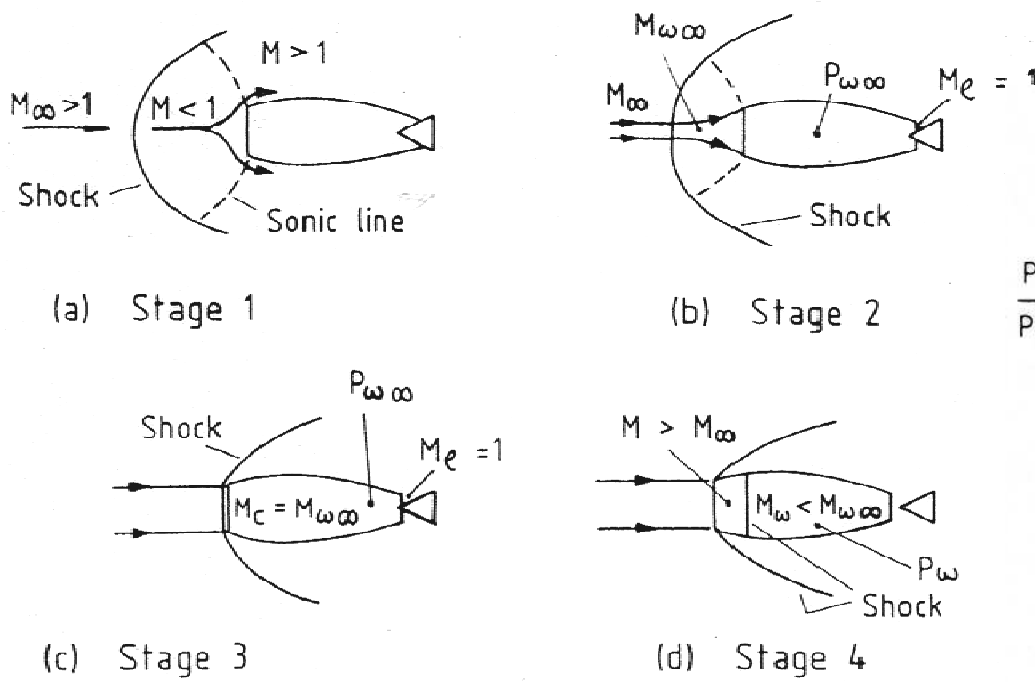

Simple supersonic Intake flow schemes

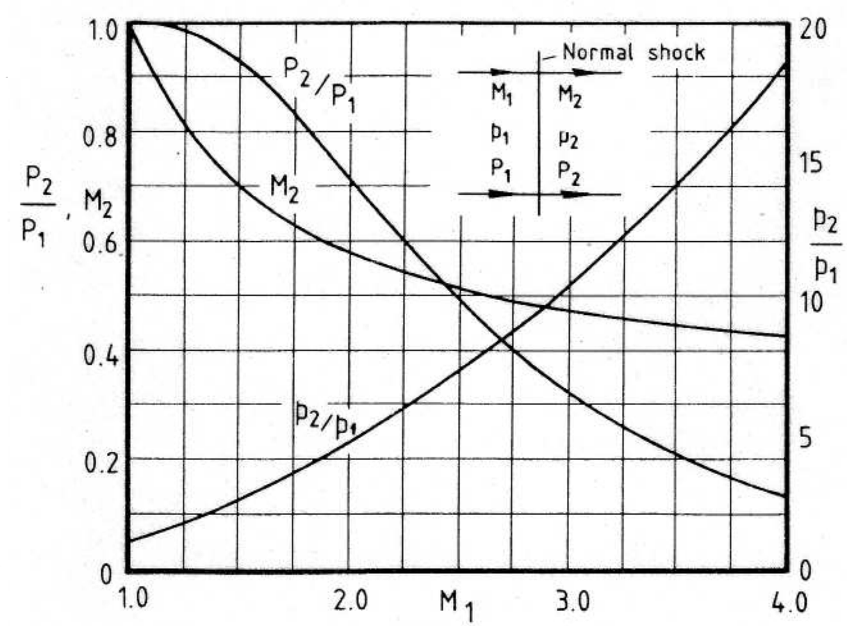

Properties of normal shock flow

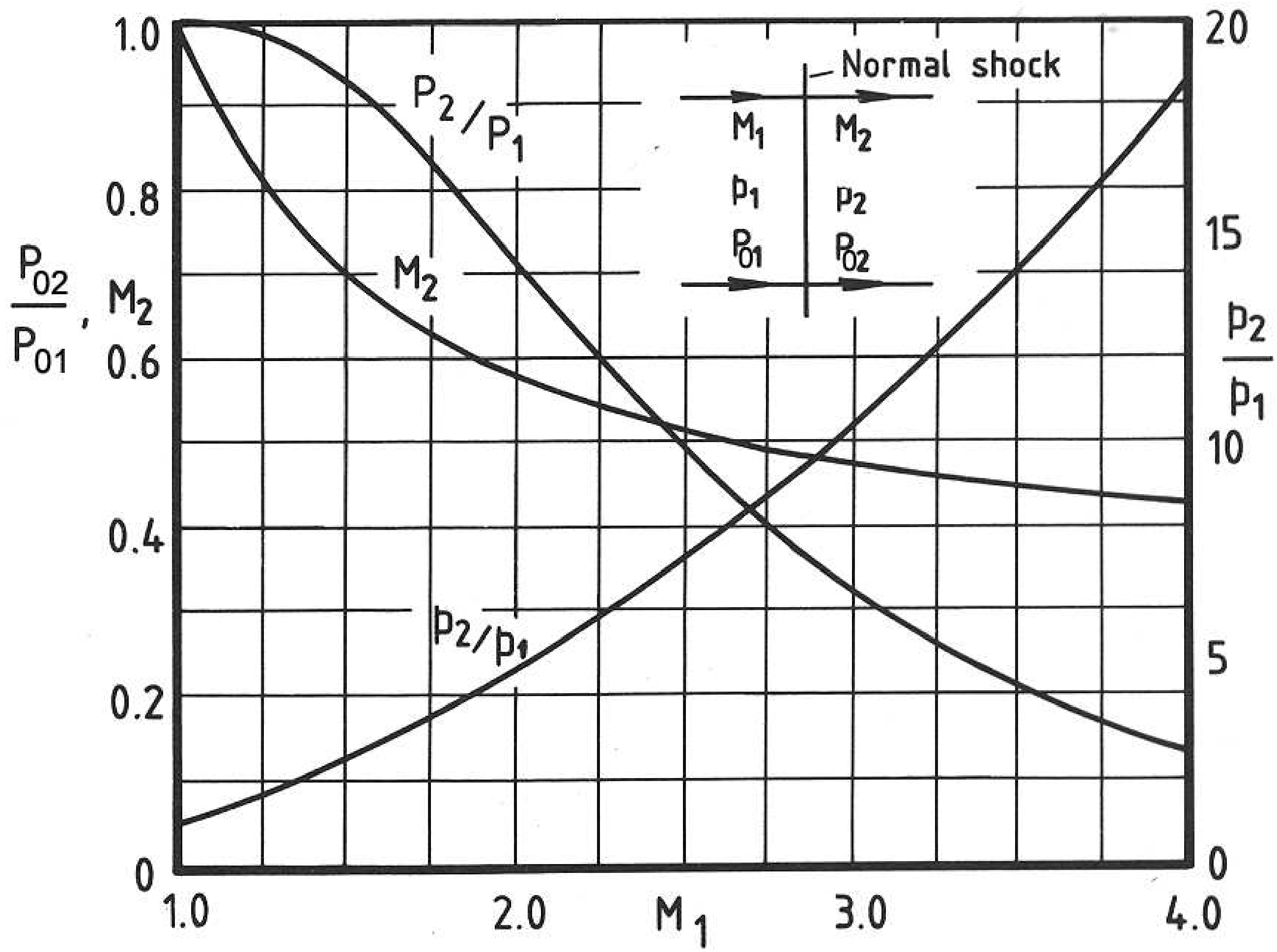

Properties of normal-shock flow

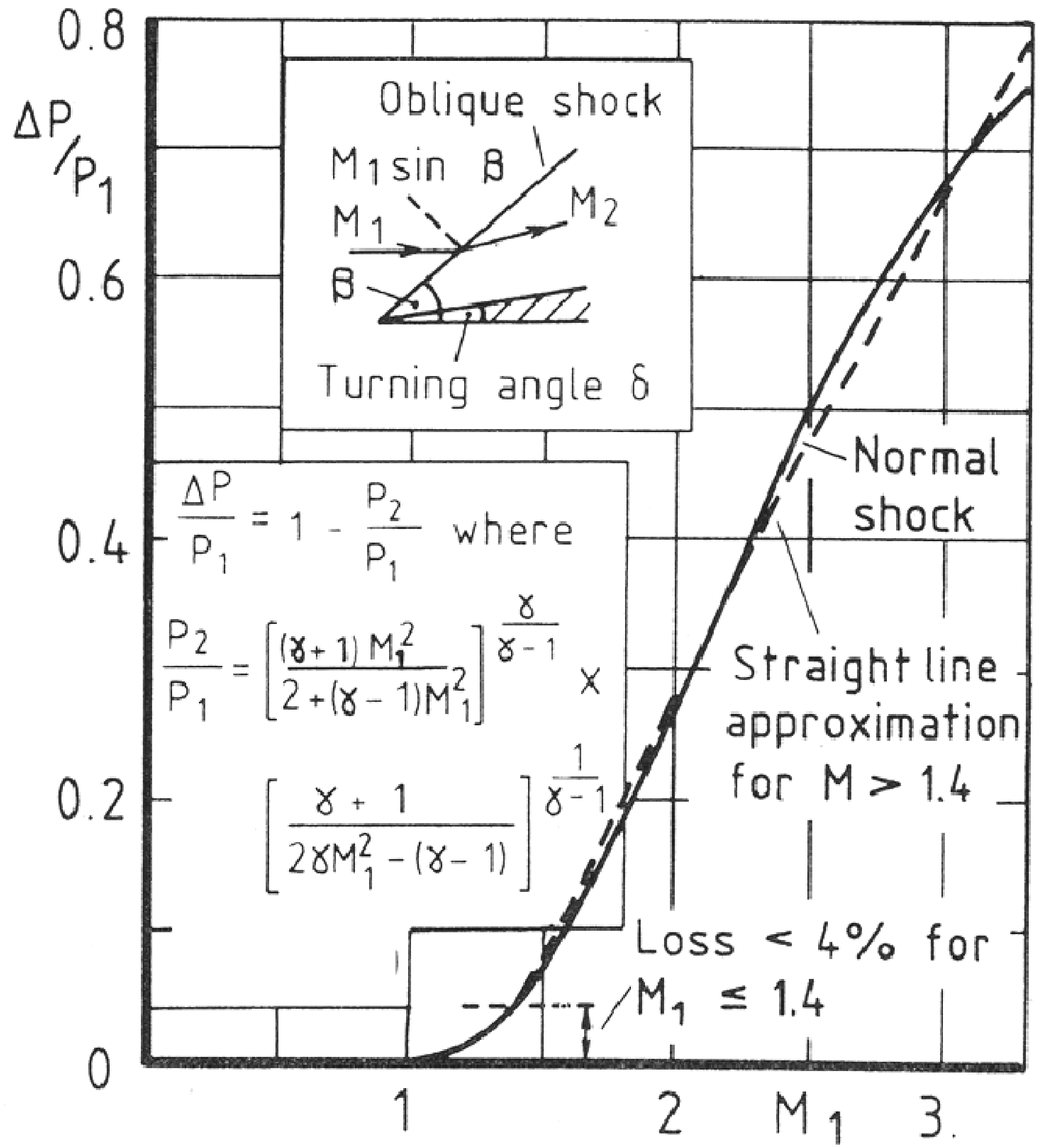

Normal shock loss and reasons for multiple oblique shocks

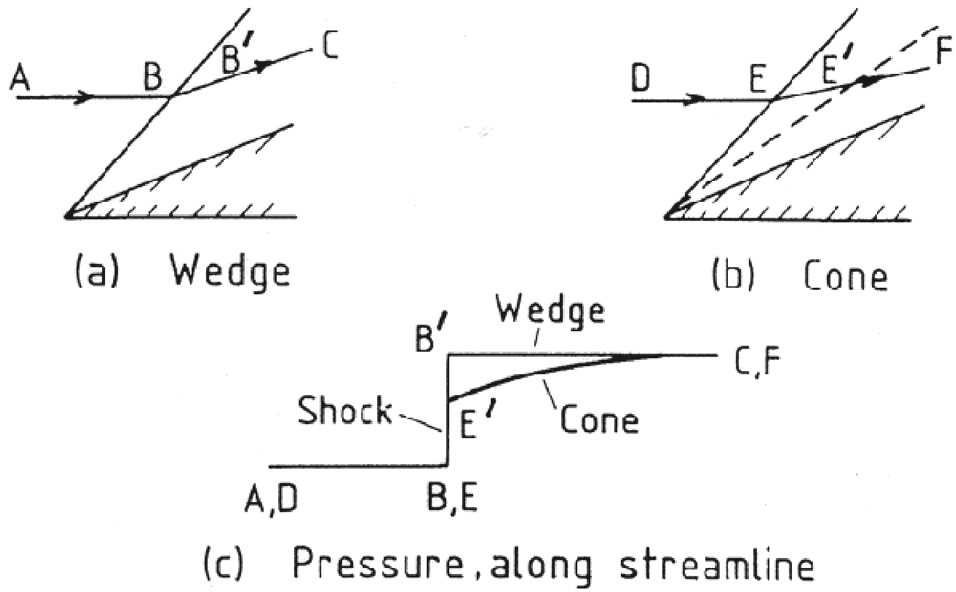

Difference between wedge and cone flow

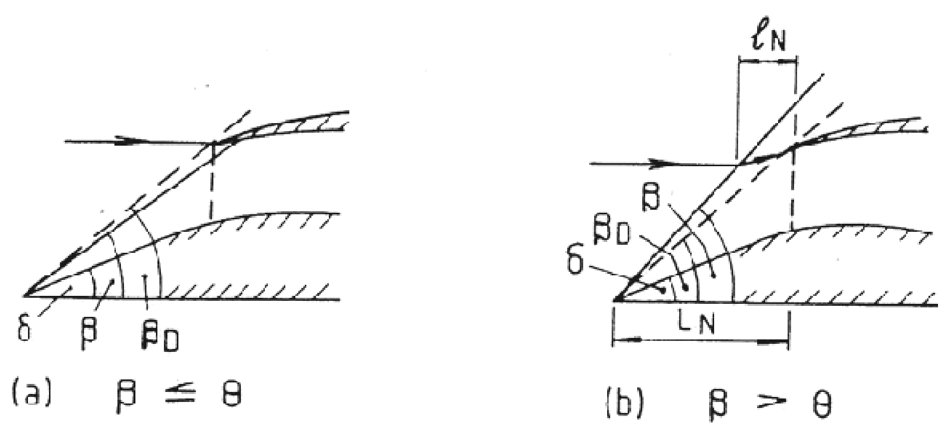

Flow conditions for s single wedge intake

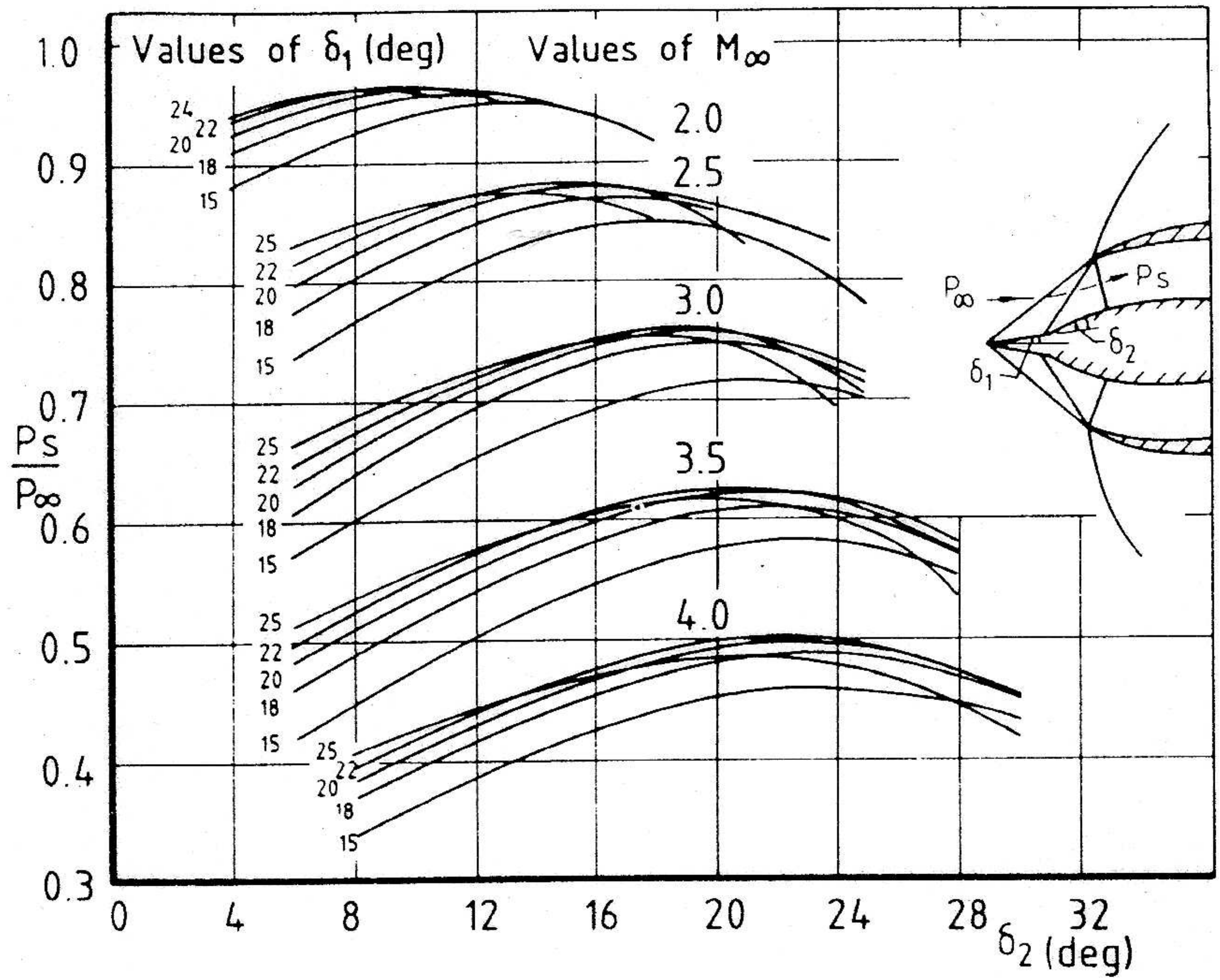

Shock recovery with double-cone Intakes

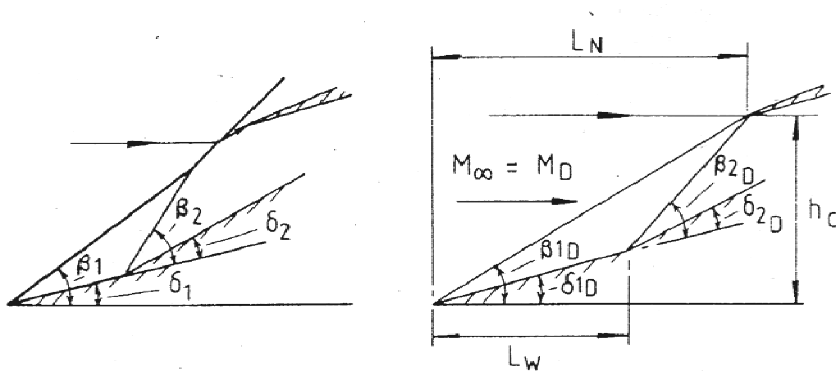

Double wedge Intake

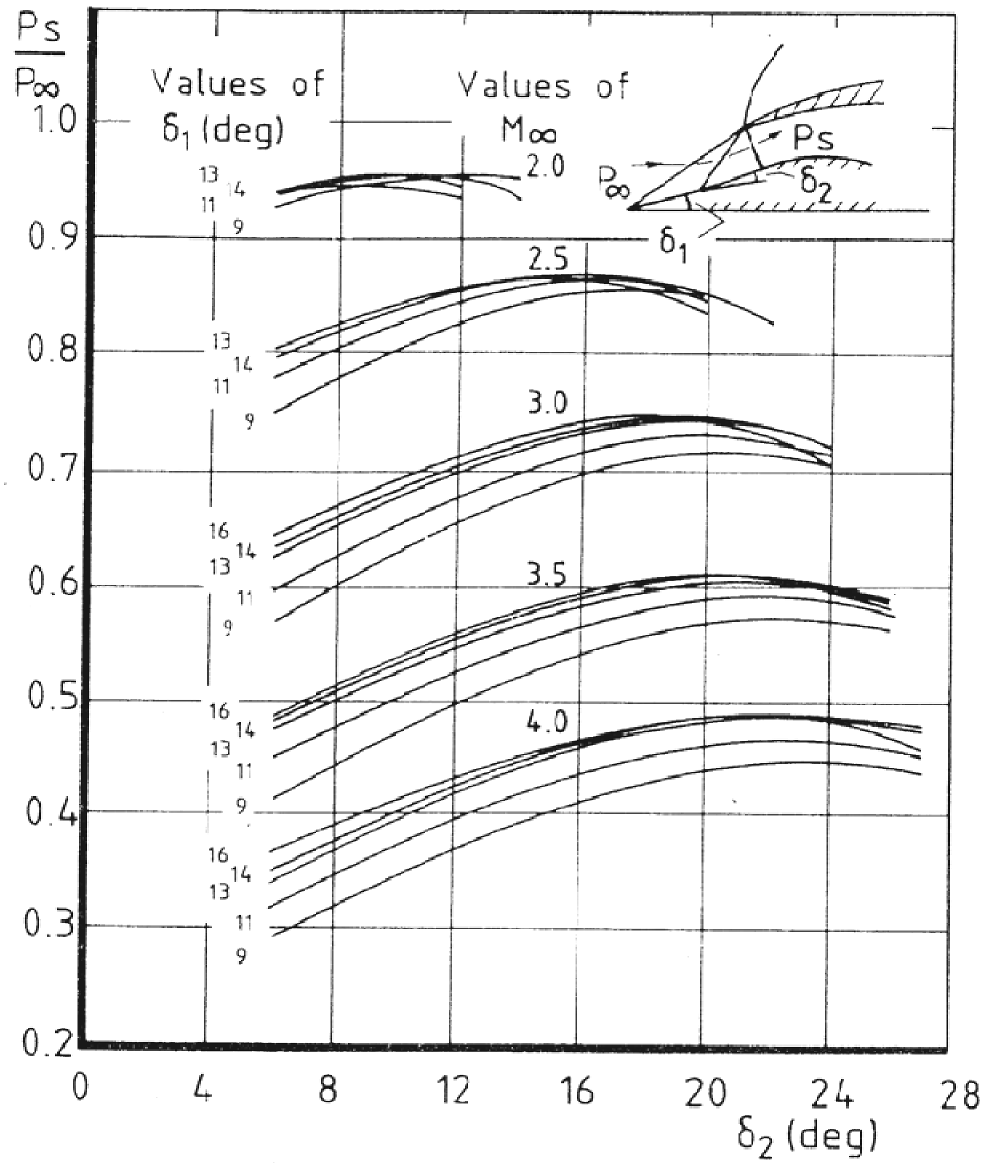

Shoch recovery of Double wedge Intakes

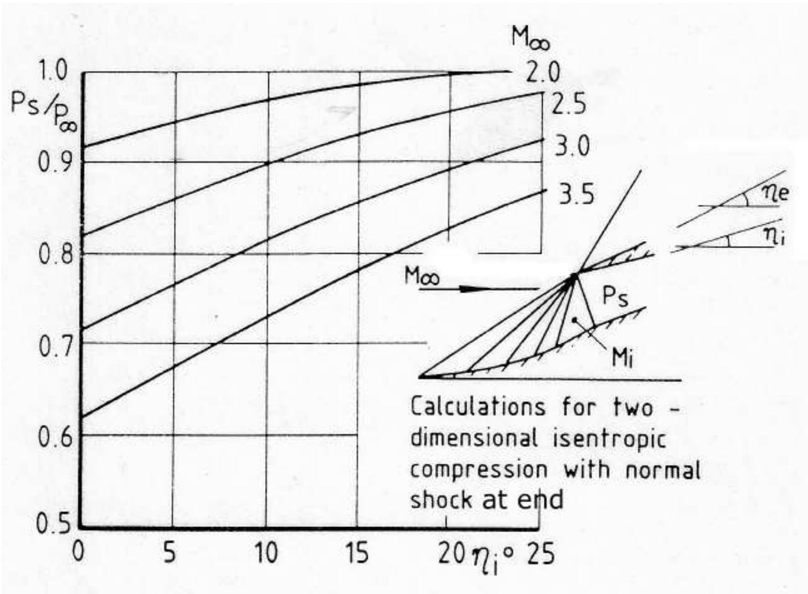

Intake Shock pressure recovery - insentropic compression

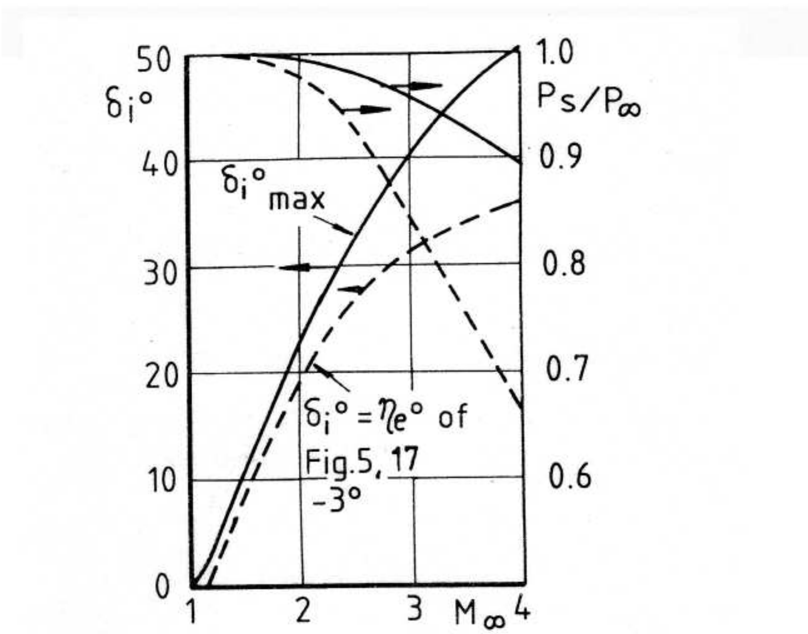

Maximum angle of isentropic forebody and corresponding pressure recovery for angled duct and η_e

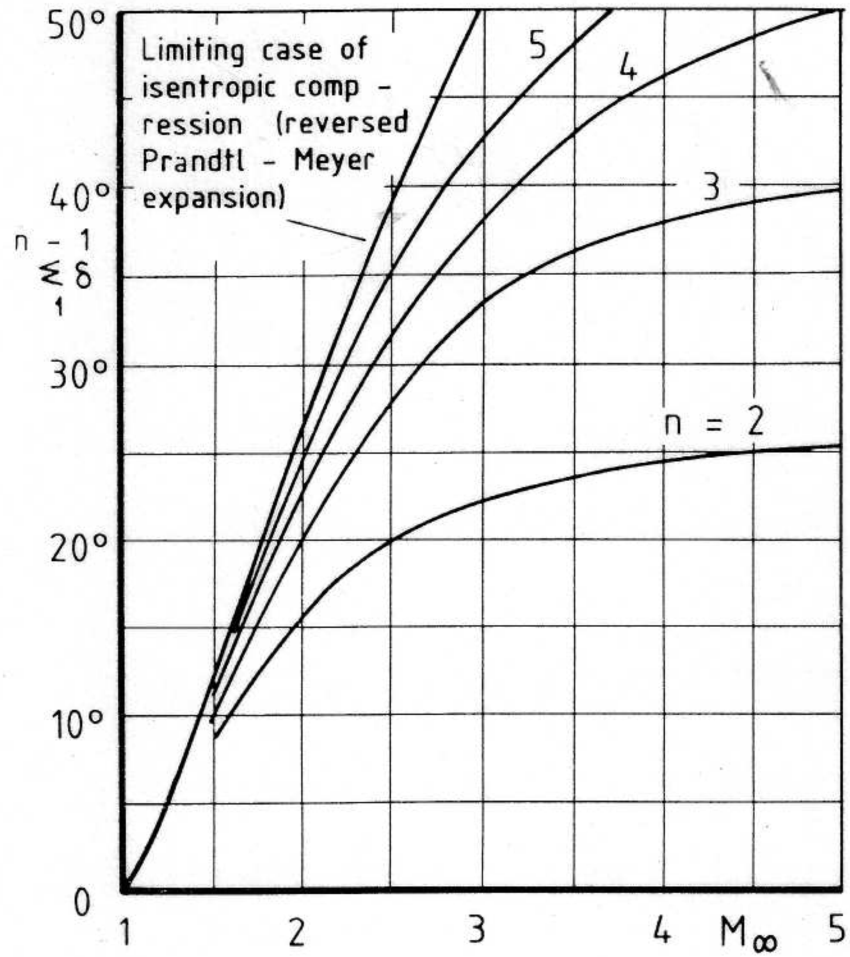

Total flow turnig angle for optimum two dimensional shocks

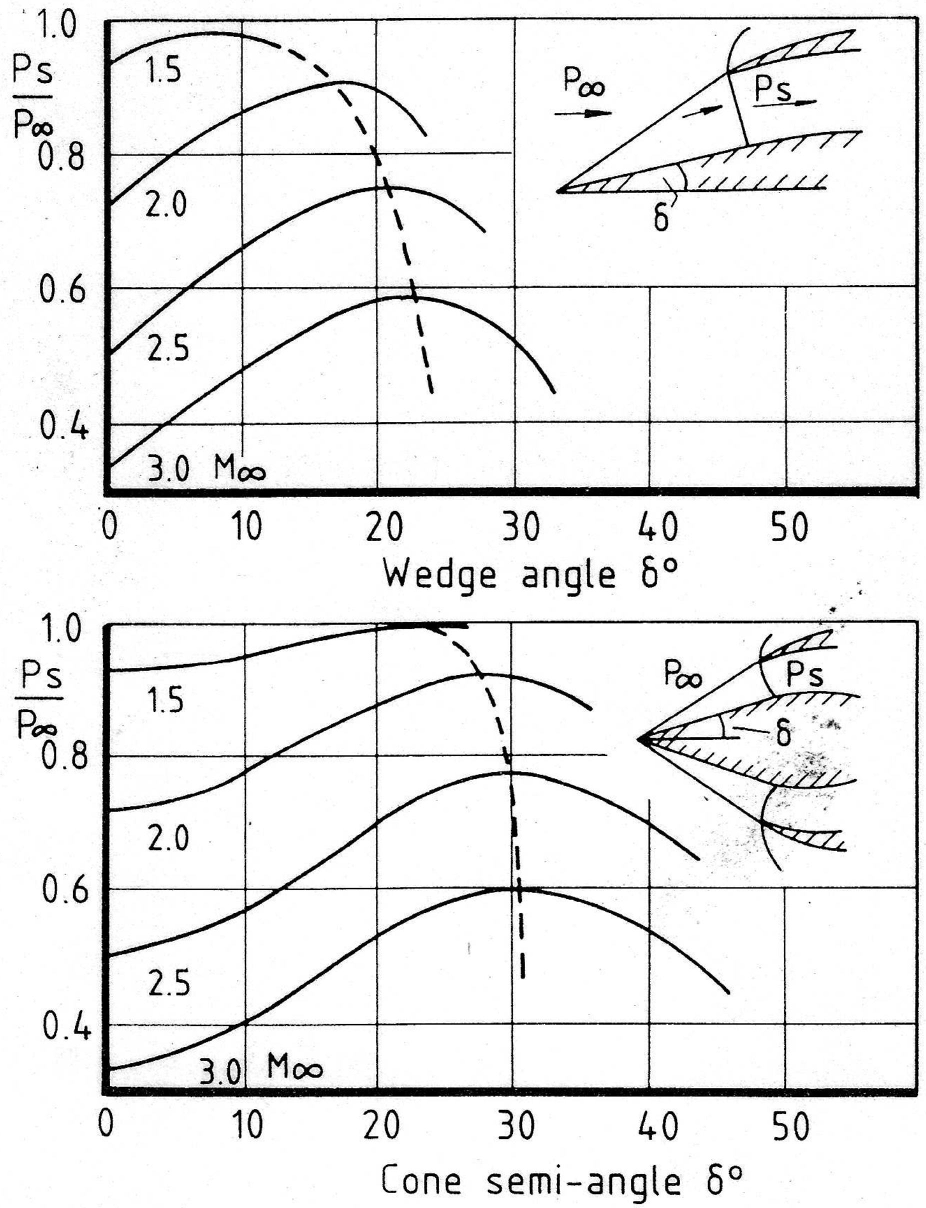

Shock recovery for wedges and cones

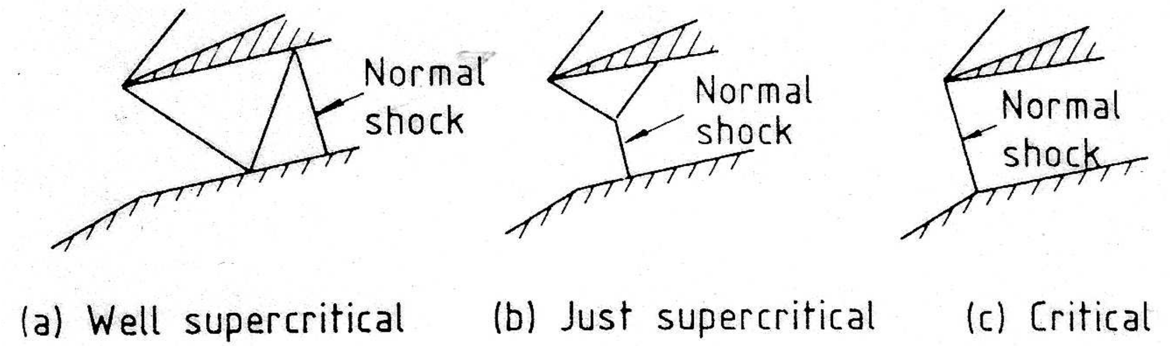

Intake Shock configurations

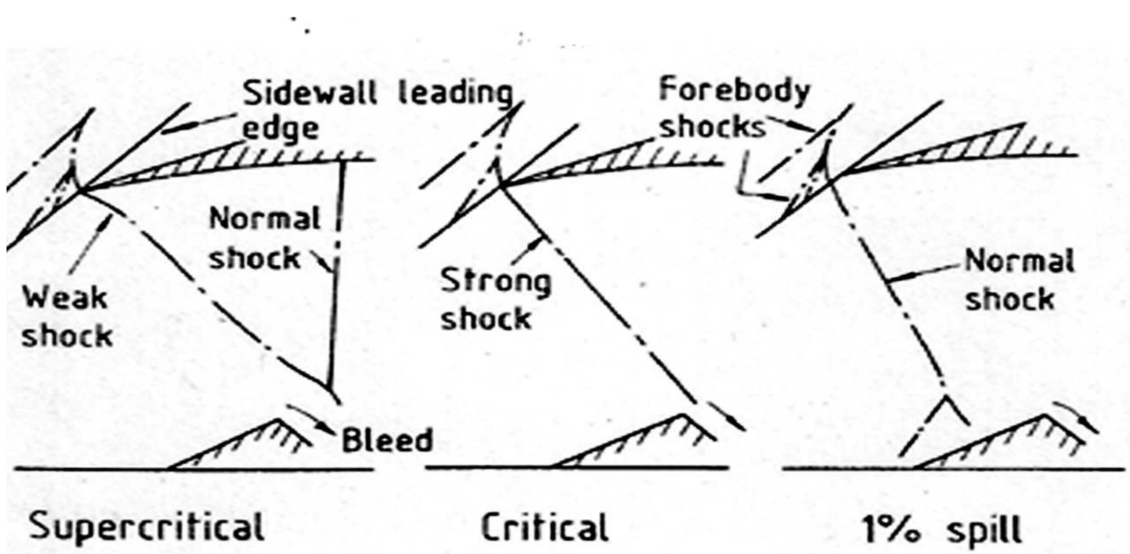

A supersonic Intake (M = 2.0) with boundary layer bleed system

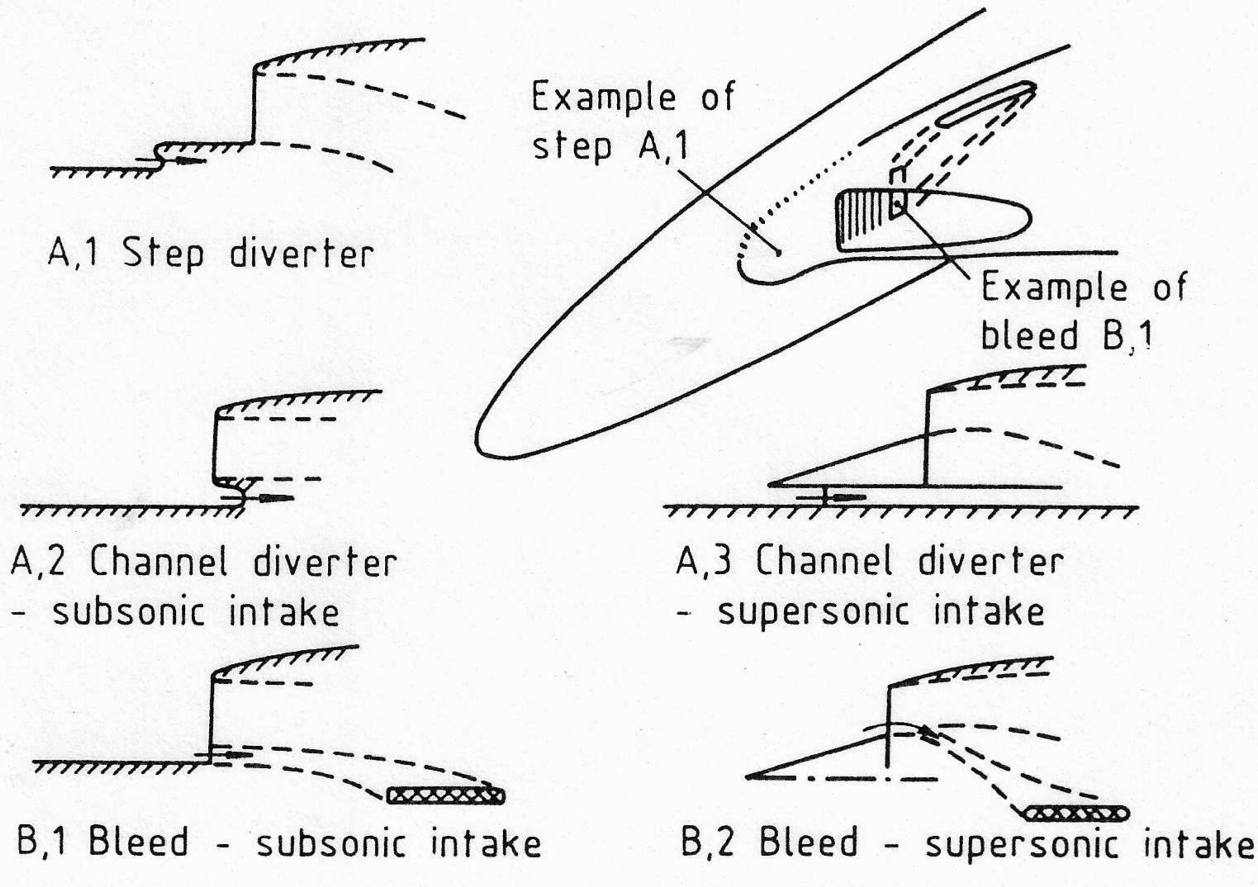

Common forms of bleed and diverter.

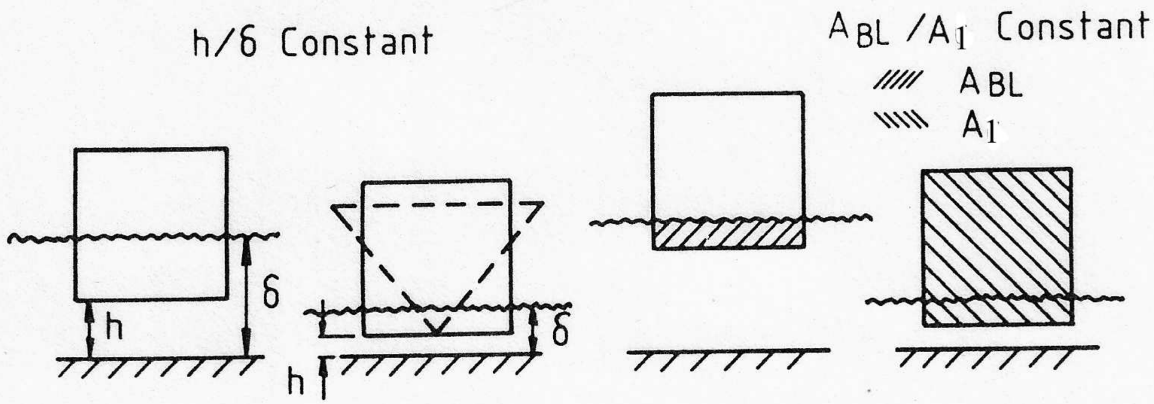

(a) Influence of intake size and shape

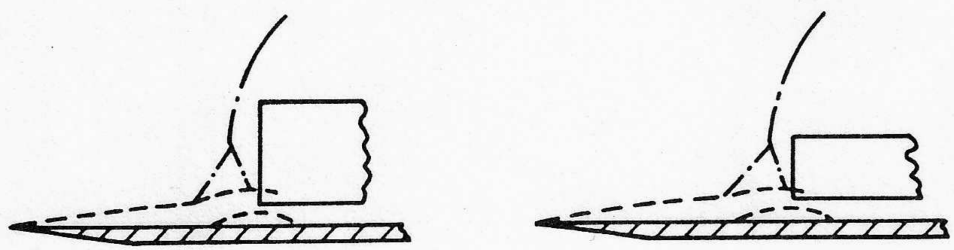

(b) Influence of scale of shock and boundary layer interaction

Problems of representation of bleed parameters.

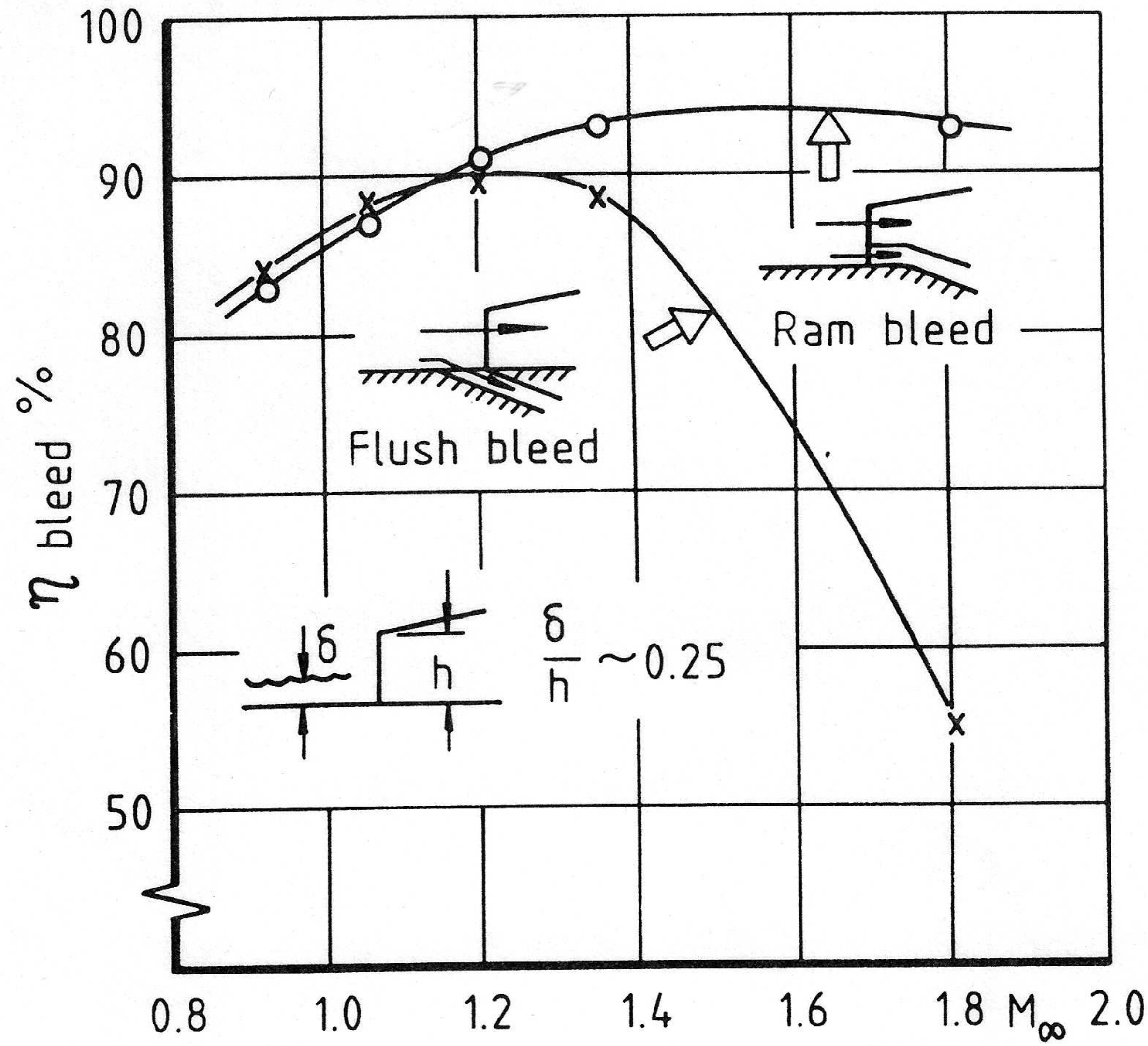

Comparative efficiencies of particular ram and flush bleeds.

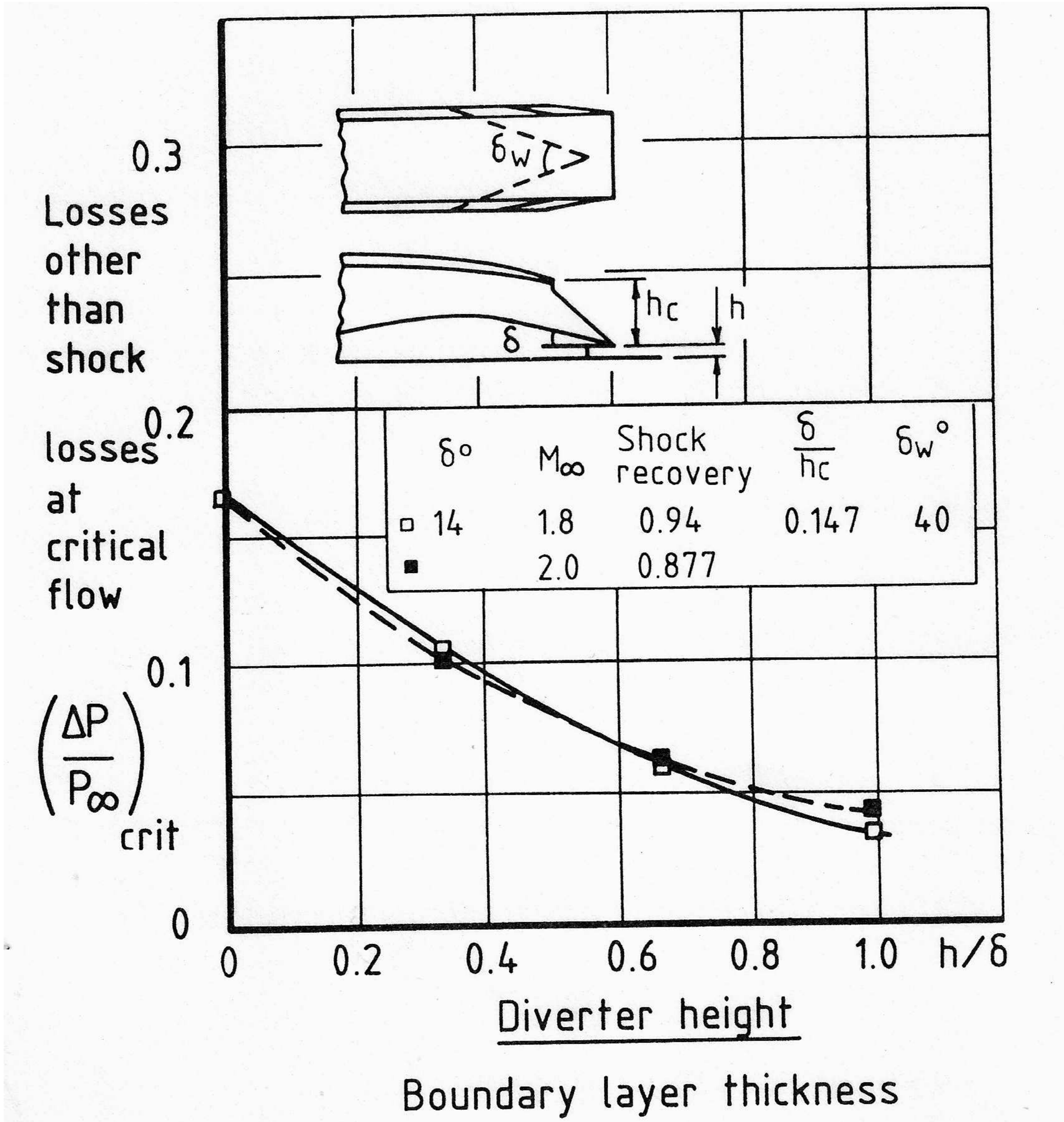

Diverter selection in supersonic intake

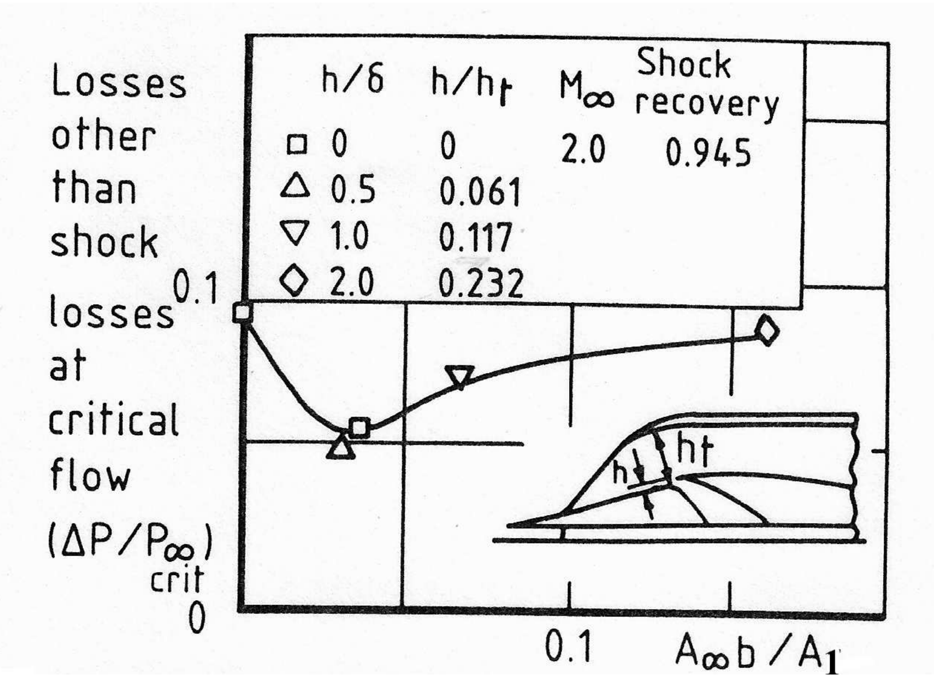

Ram scoop bleed in supersonic intake

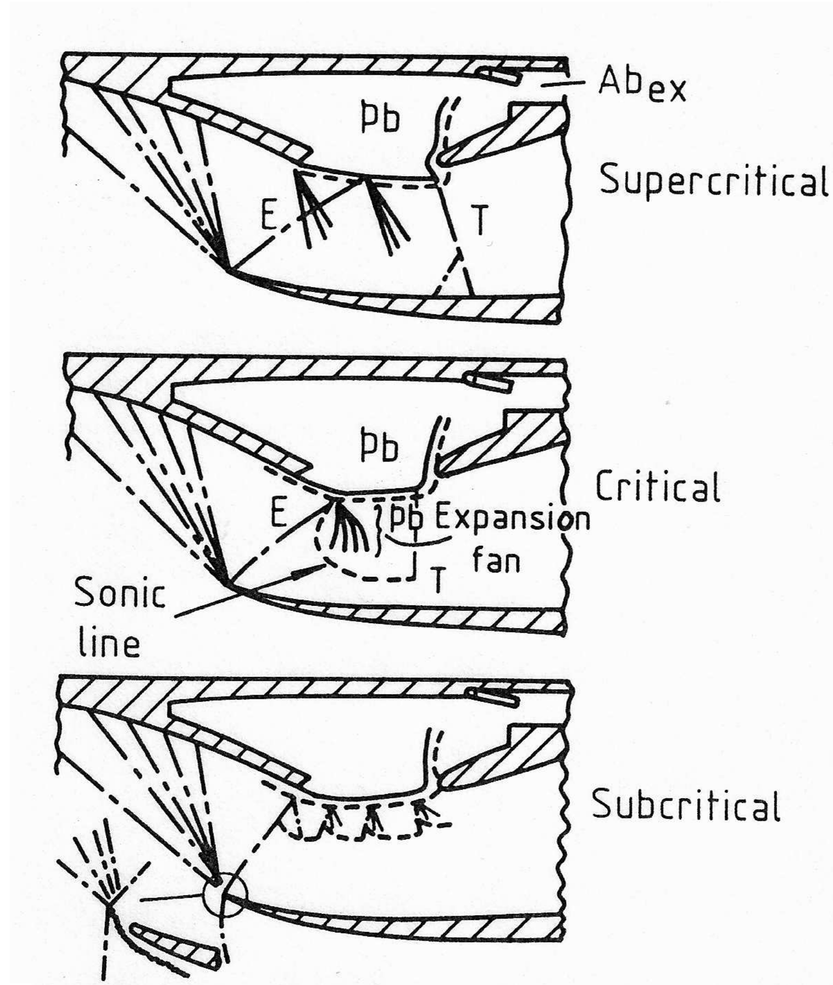

Intake with flush throat bleed

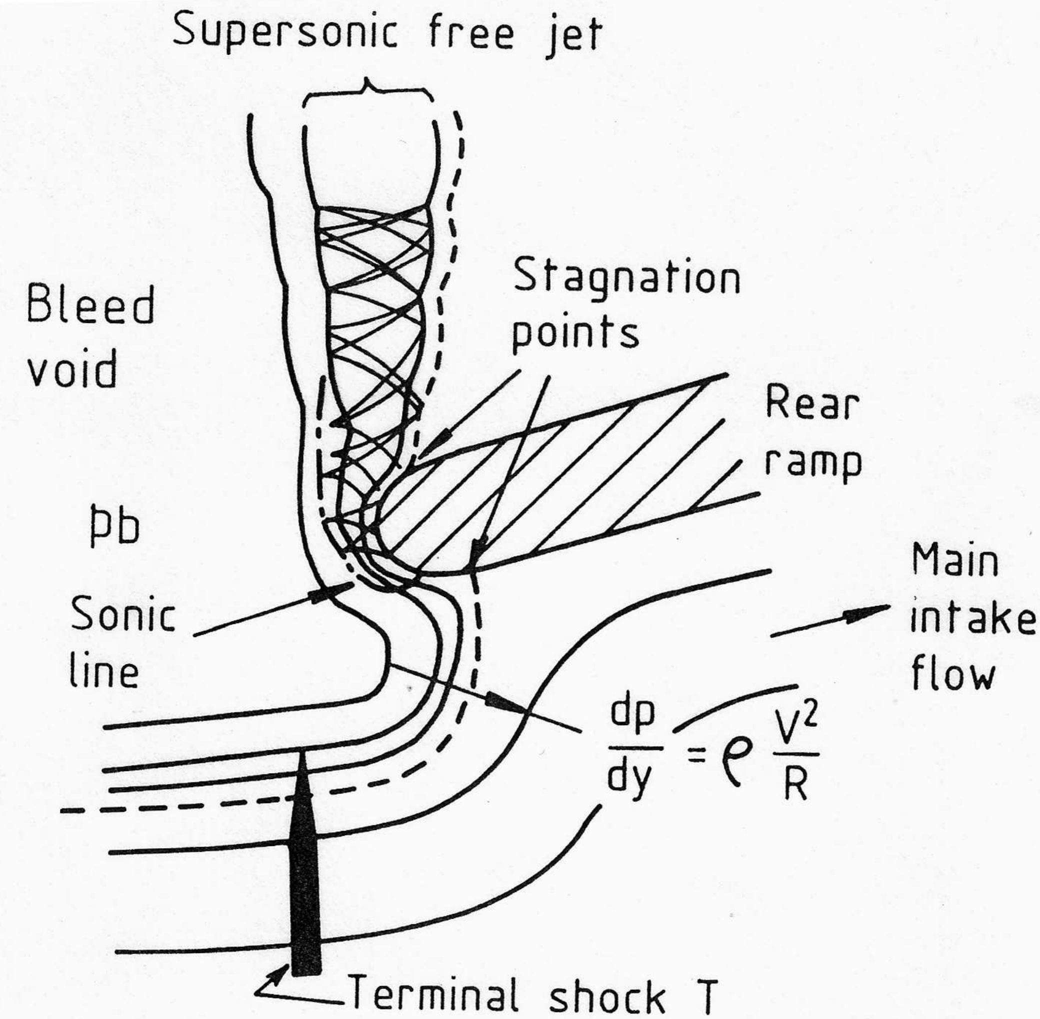

Flow pattern in vicinity of rear lip of a wide flush bleed.

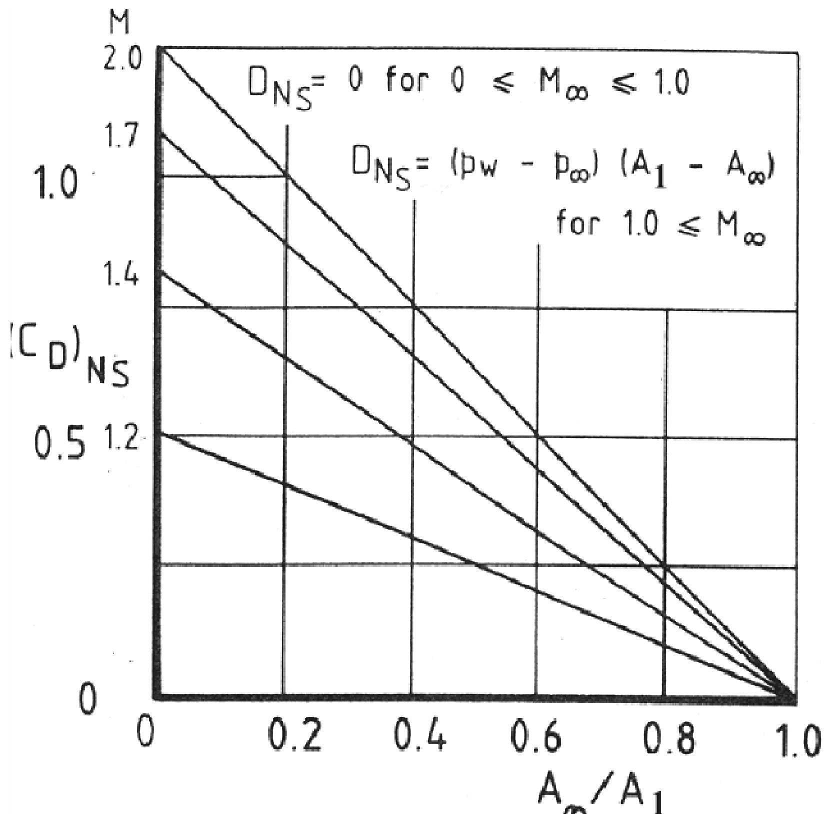

Variation of normal-shock drag coefficient with flow ratio and free stream Mach number.

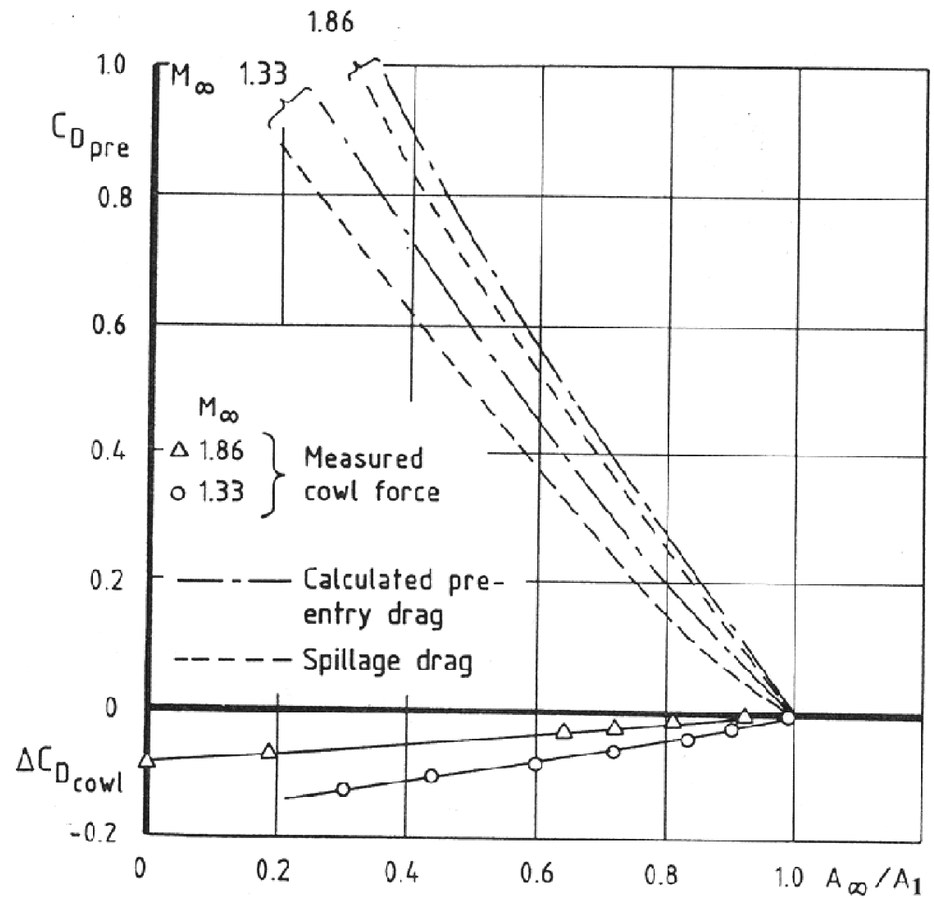

Variation of spillage drag, pre-entry drag and change in cowl force with flow ratio

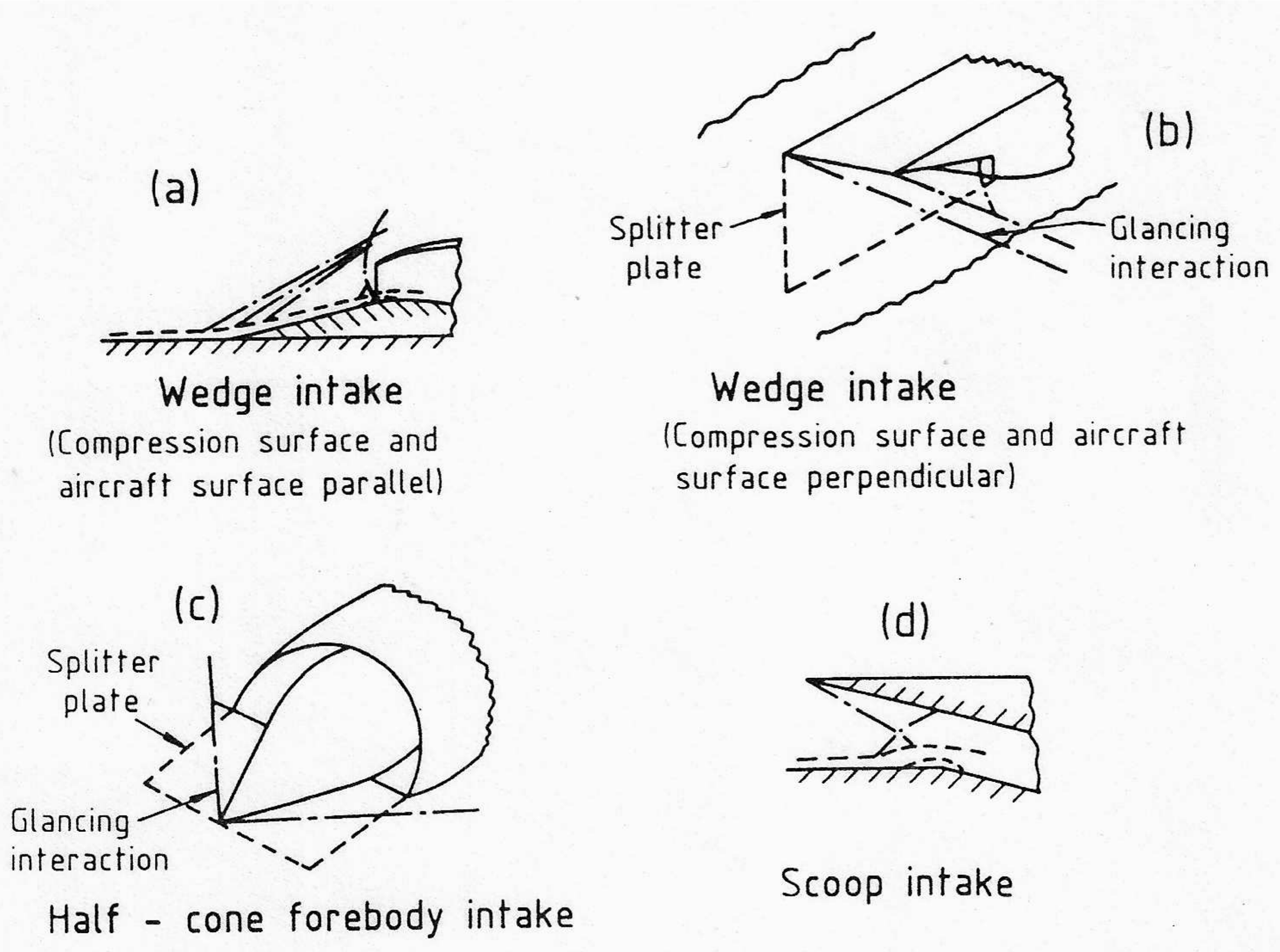

Shock and boundary layer interactions for intakes with compression surfaces.

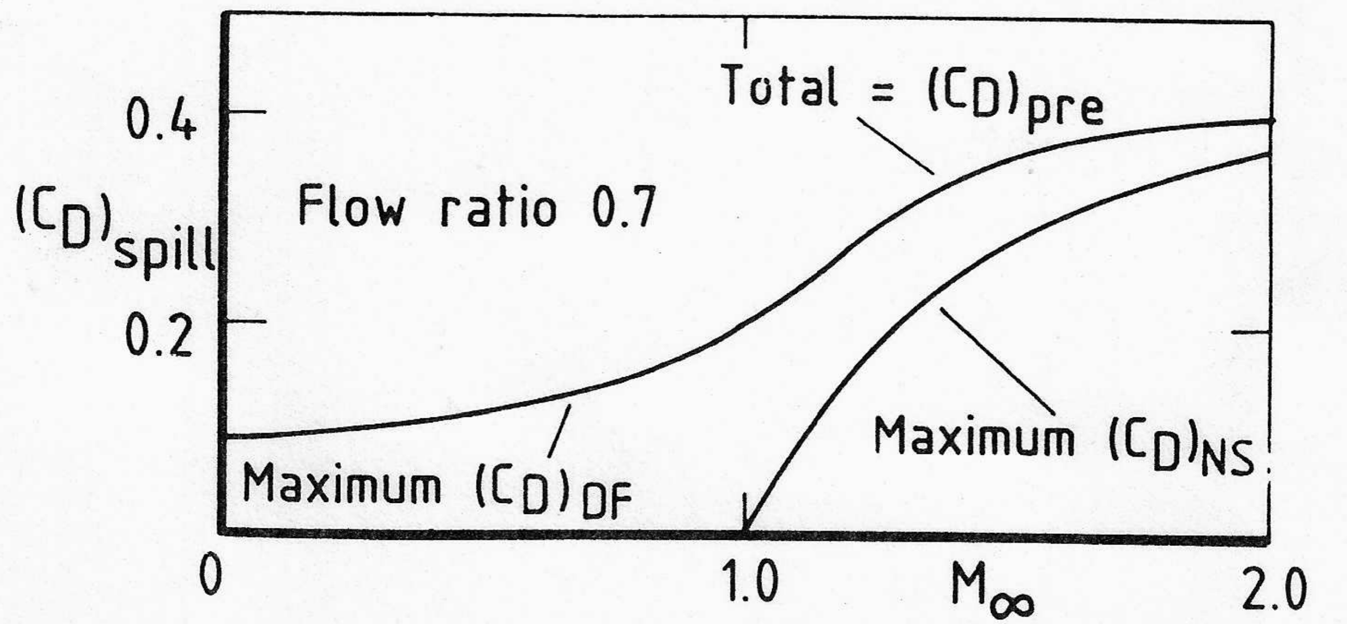

Variation of maximum disturbed-flow drag and maximum normal-shock drag at constant flow ratio.

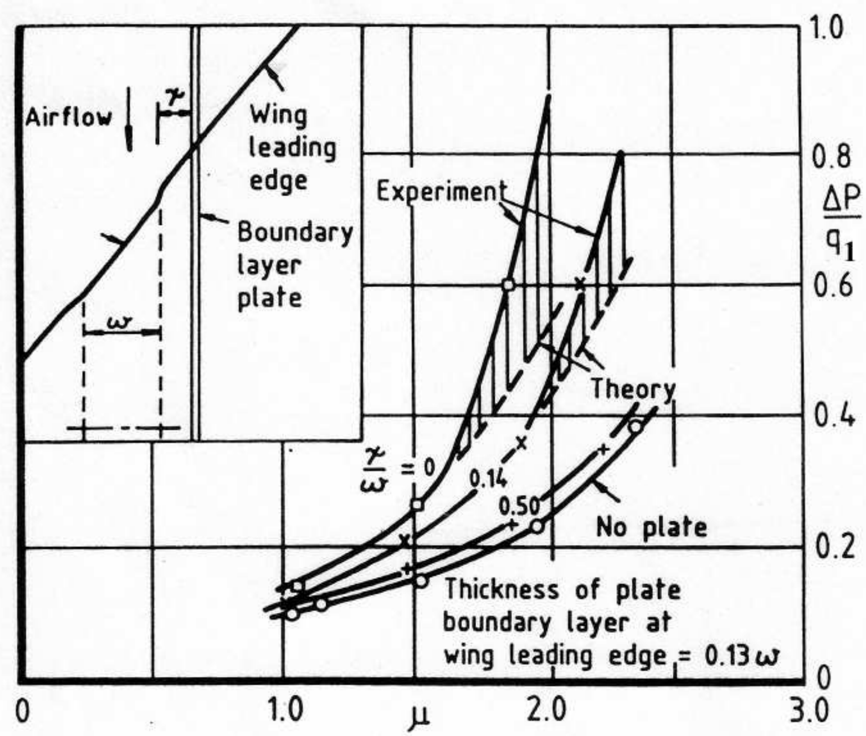

Intakes: pre-entry flow separation.

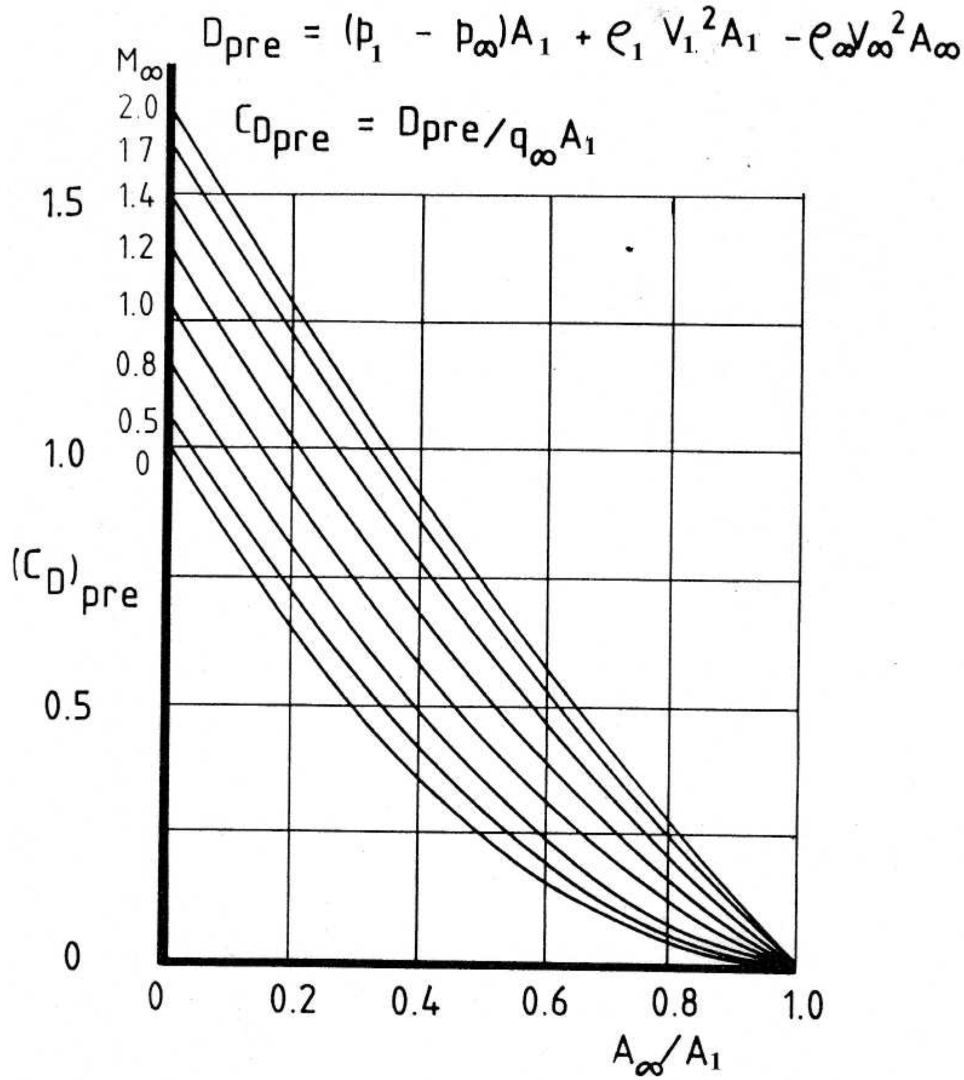

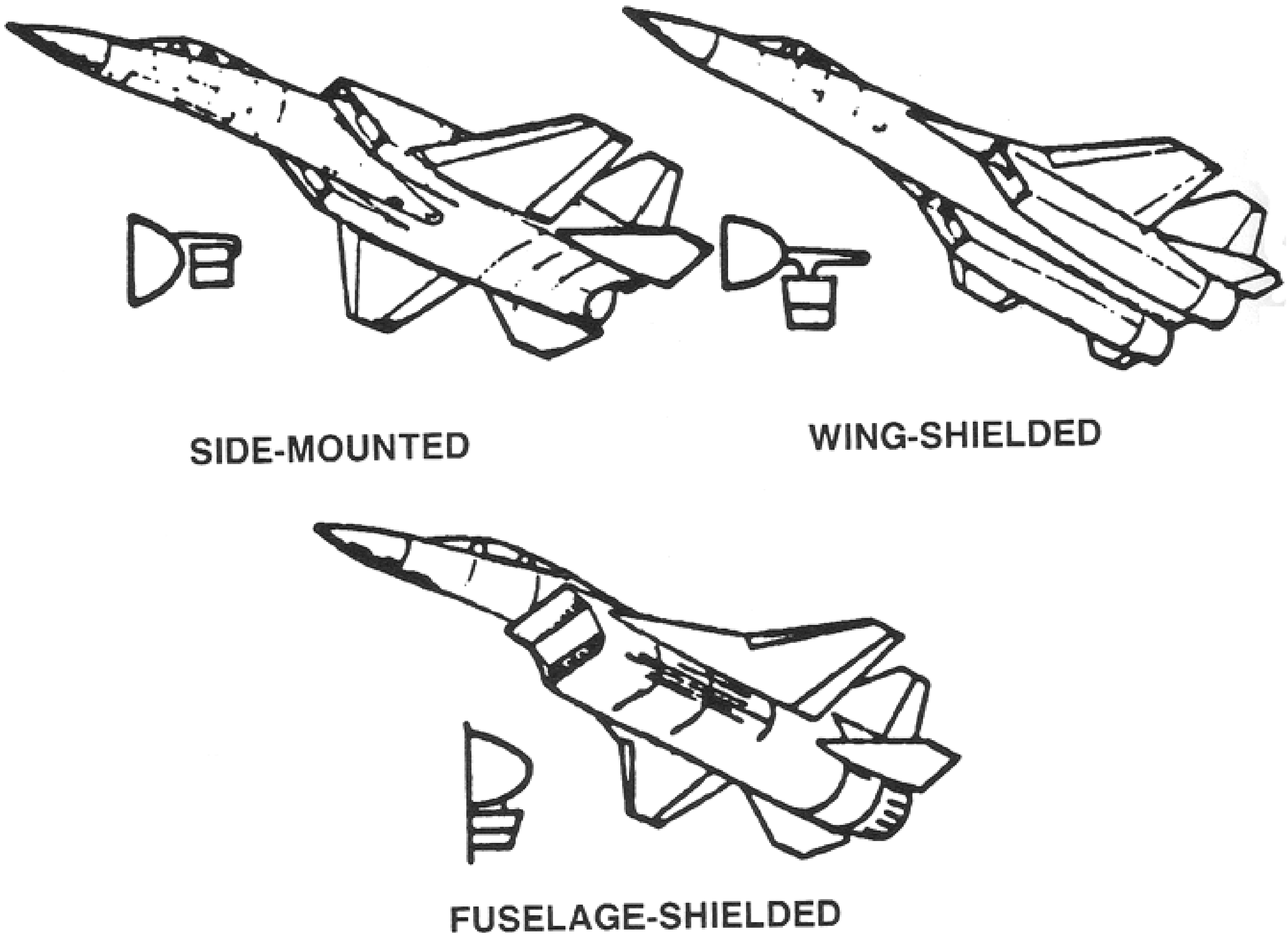

Three Inlet Locations

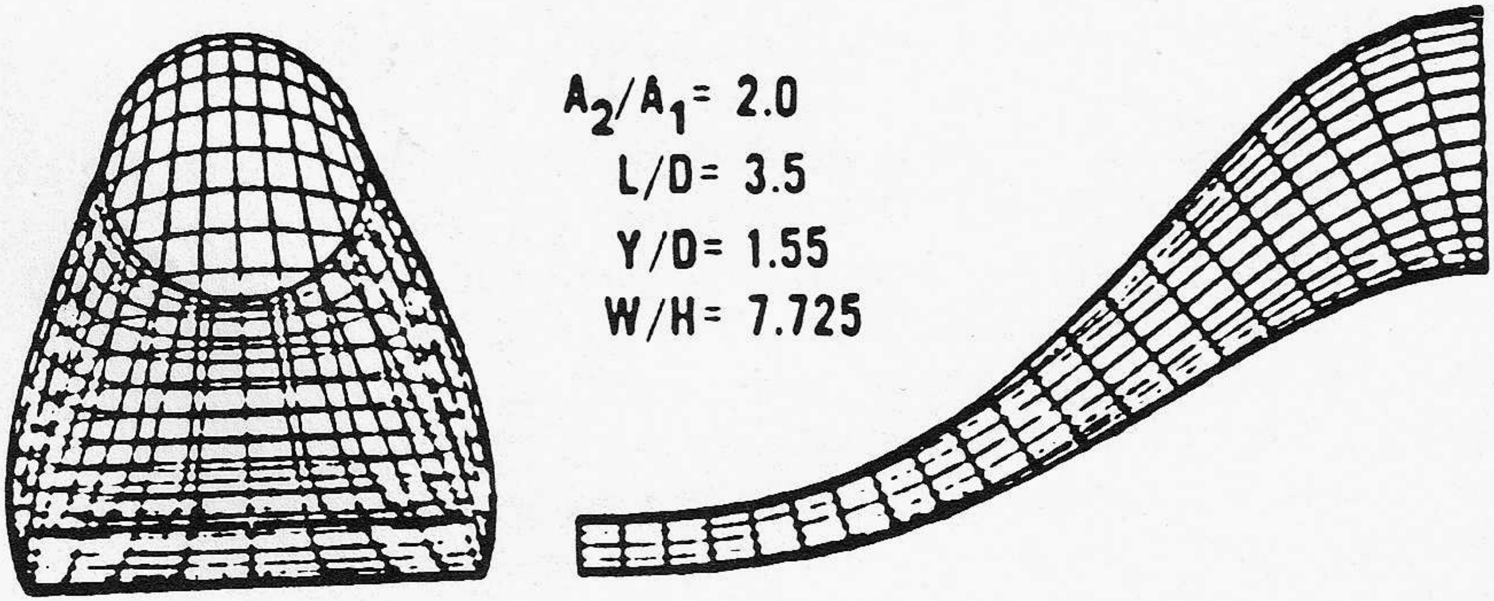

Typical Diffuser Portion of Supersonic Inlet

Nozzle Design Details

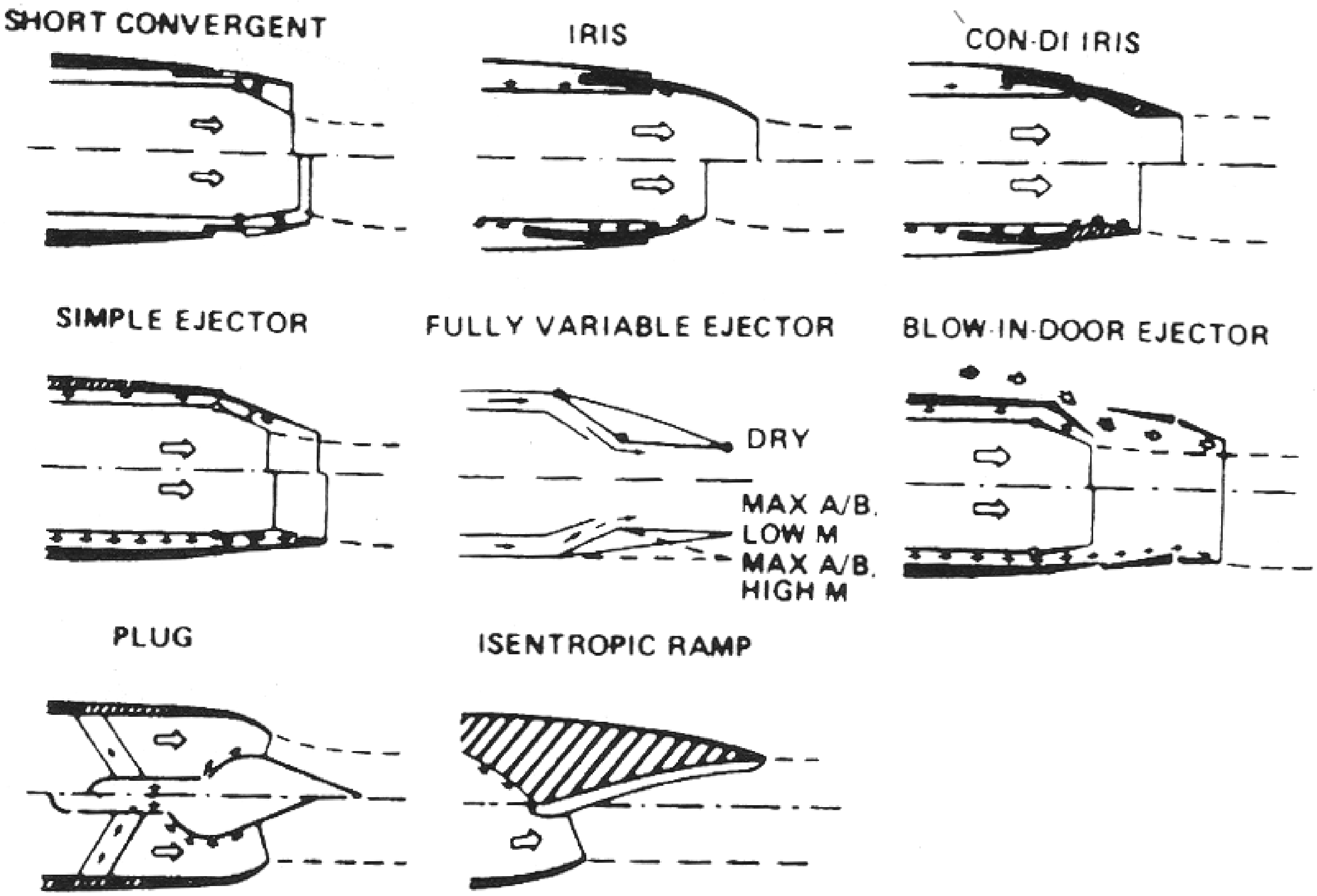

(Short arrows indicate the presence and flow direction of nozzle cooling air which is usually inlet bleed air, compressor bleed air, or fan discharge air)

Typical Nozzle Concepts for Afterburning Engines

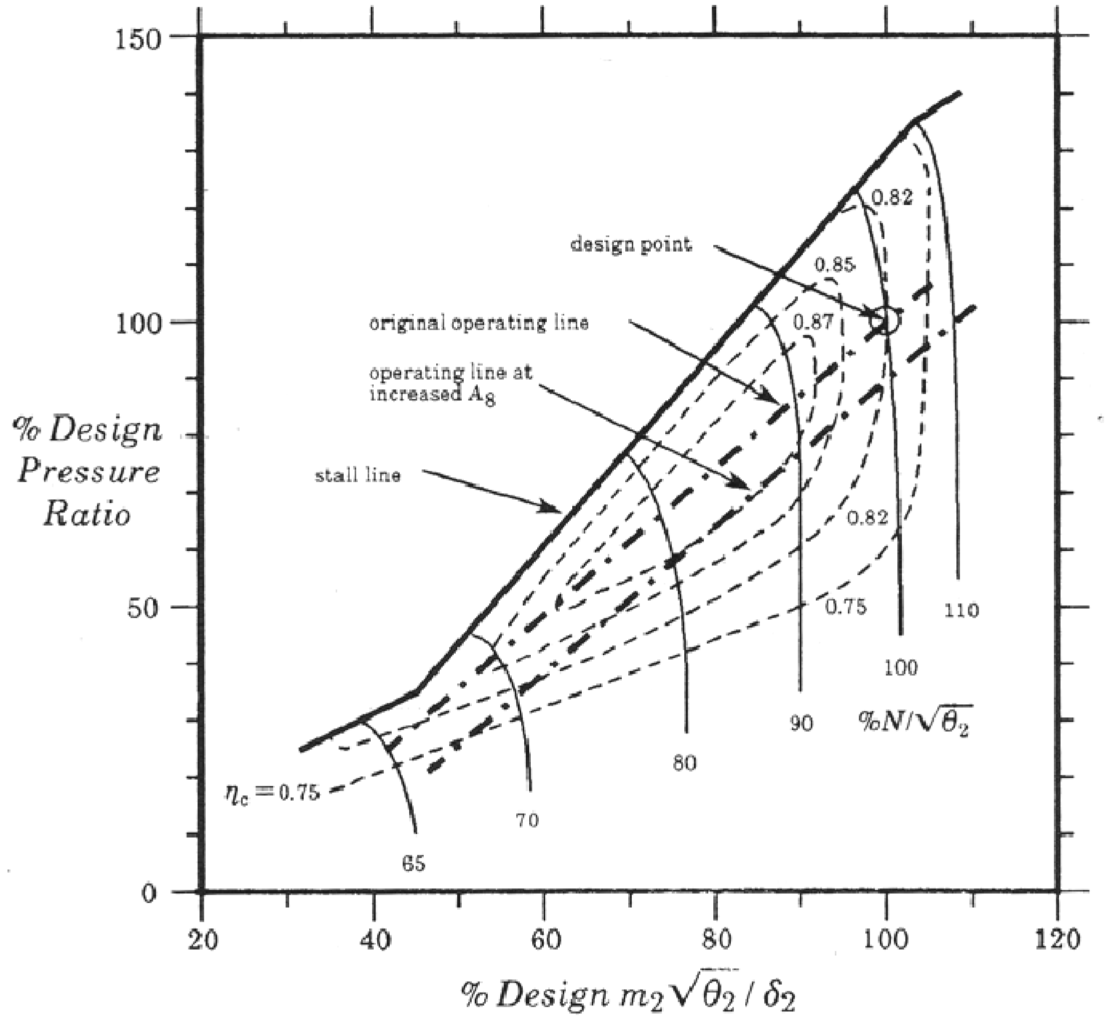

Compressor Map flixibility with Variable geometry nozzle configuration

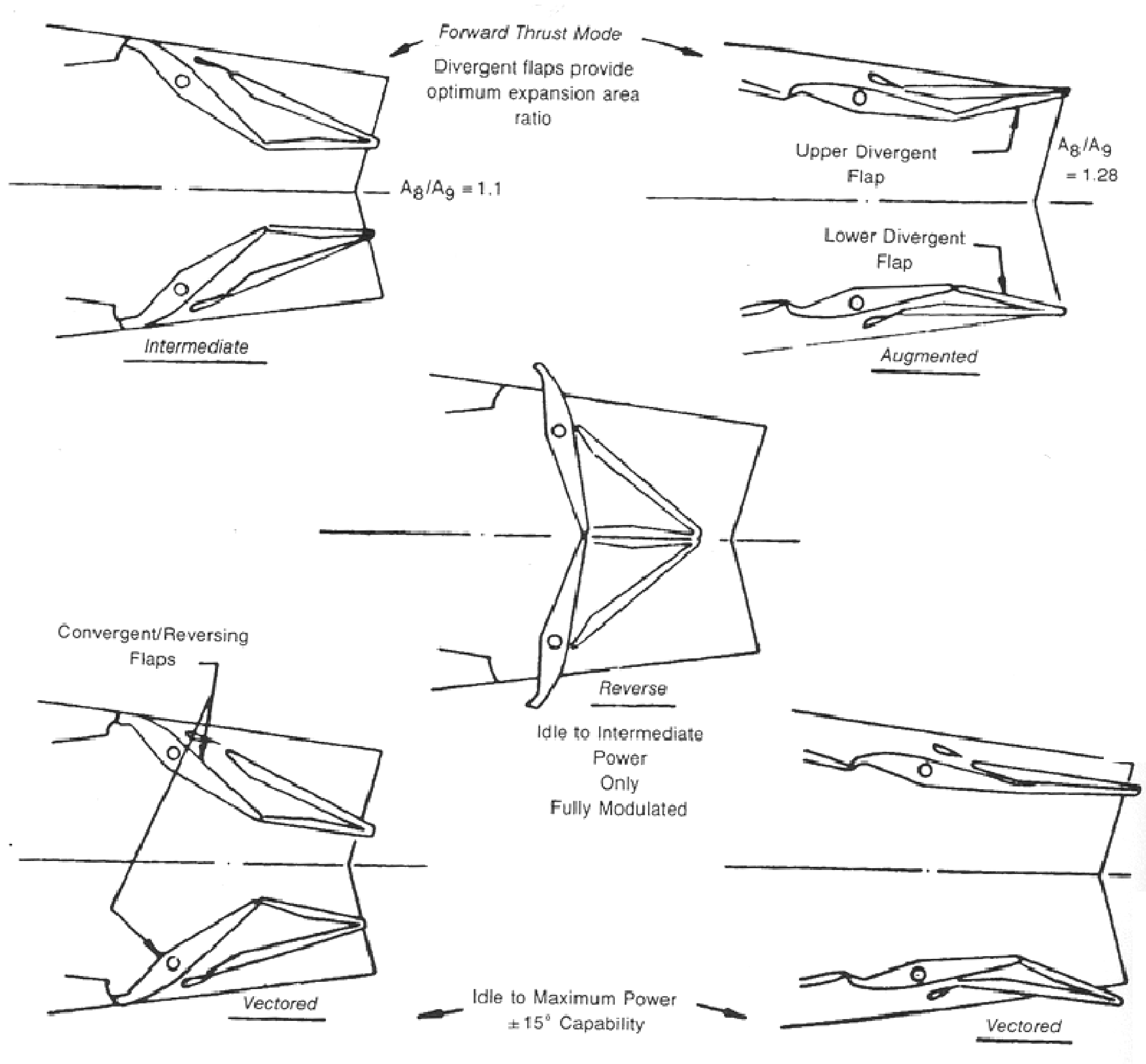

Typical Two-Dimensional Thrust Vectoring Nozzle with Thrust Reversing

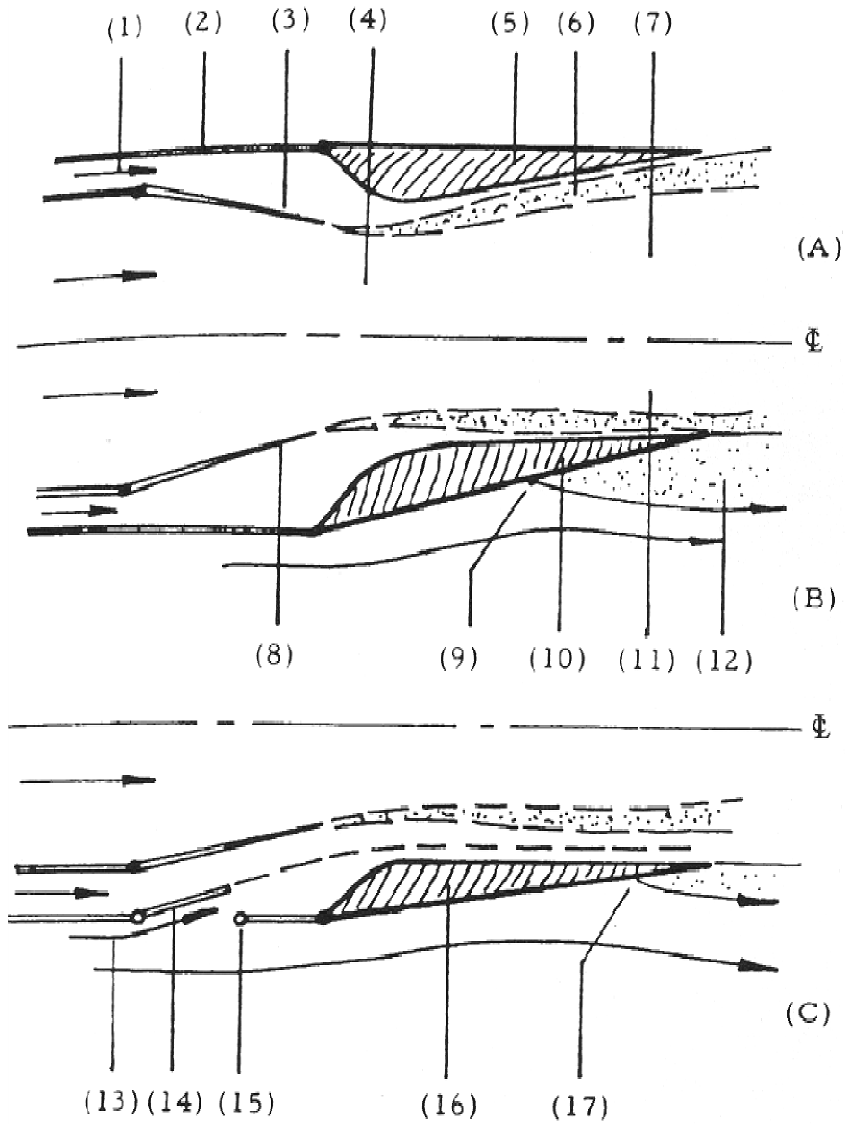

(A) Supersonic nozzle configuration with afterburning: (1) secondary flow, (2) outer case of engine, (3) movable primary nozzle shown at maximum area, (4) primary flow, effective throat, (5) movable secondary nozzle shown at maximum exit area, (6) mixing layer between primary and secondary streams, and (7) supersonic primary flow.

(B) Subsonic nozzle configuration with no afterburning: (8) primary nozzle at minimum area, (9) separation point of external flow, (10) secondary nozzle at minimum area, (11) sonic primary stream, and (12) region of separated flow in external flow.

(C) Subsonic nozzle configuration, no afterburning and blow-in door in use: (13) tertiary flow of ambient gas into nozzle, (14) blow-in door, inflow configuration, (15) reversible hinge/latch, (16) movable secondary nozzle, and (17) separation point of extermal flow.

Ejector Nozzle Configuration

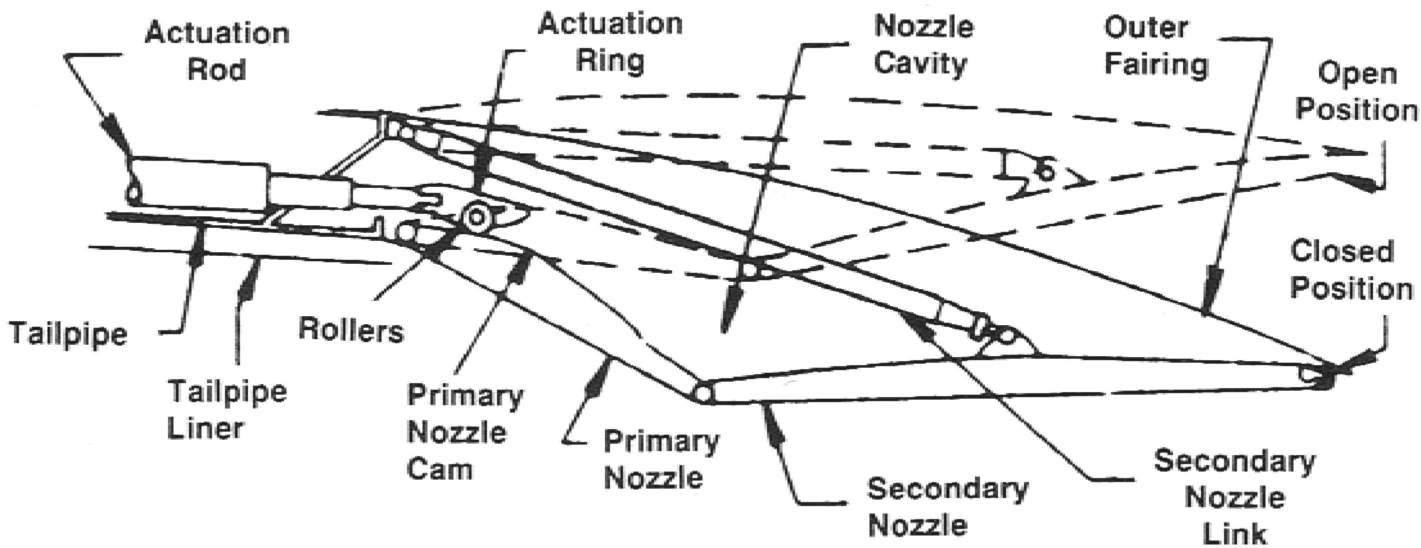

Convergent-Divergent (C-D) Exhaust Nozzle Schematic

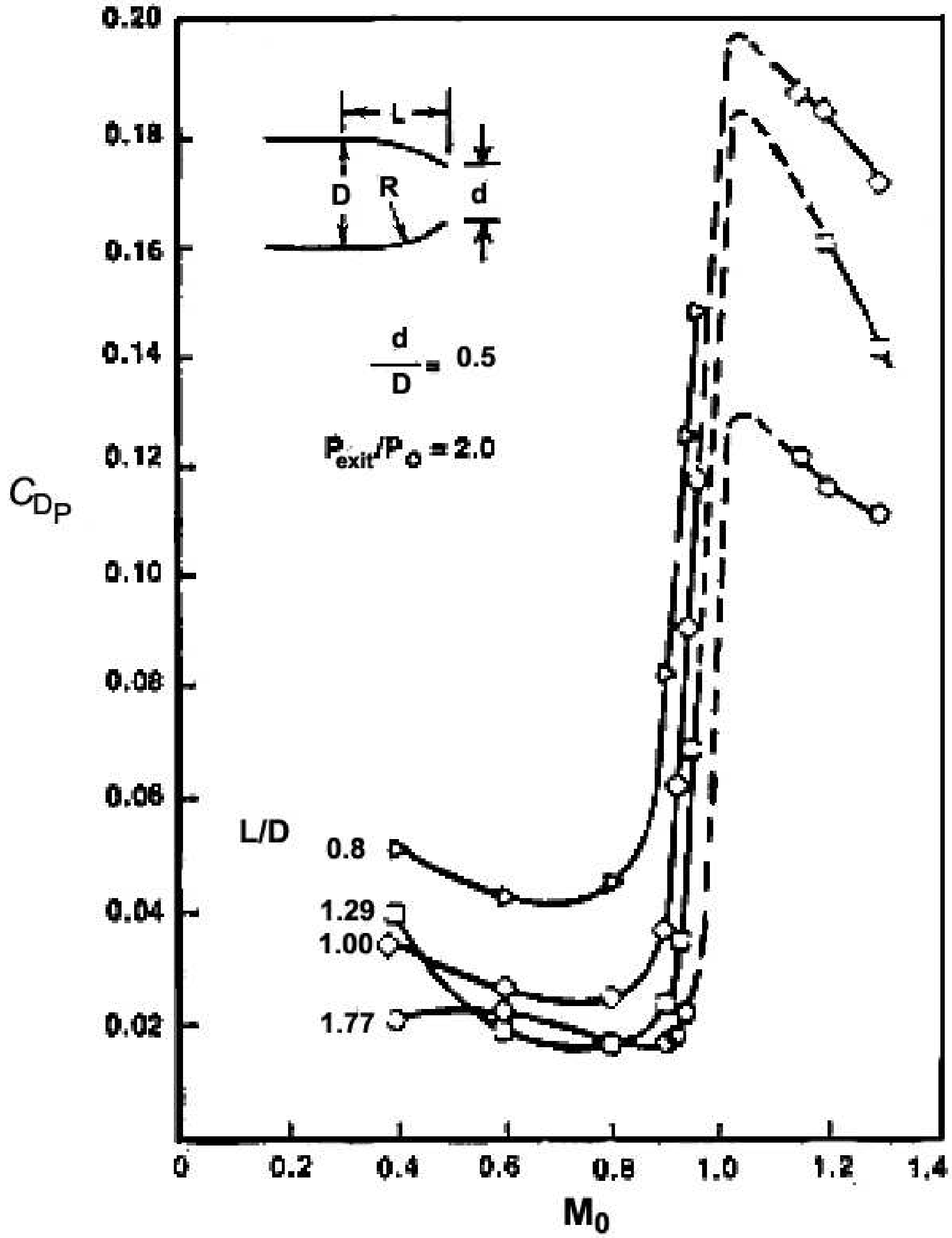

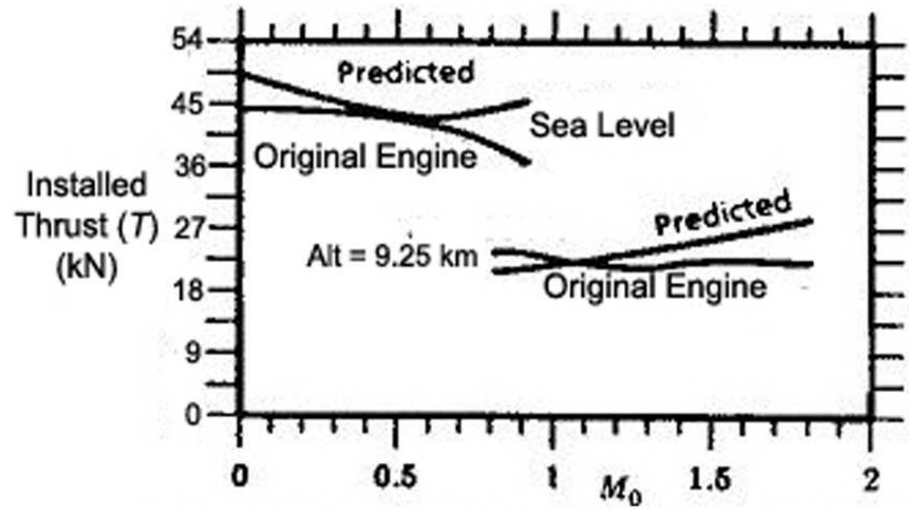

Boat Tail Drag

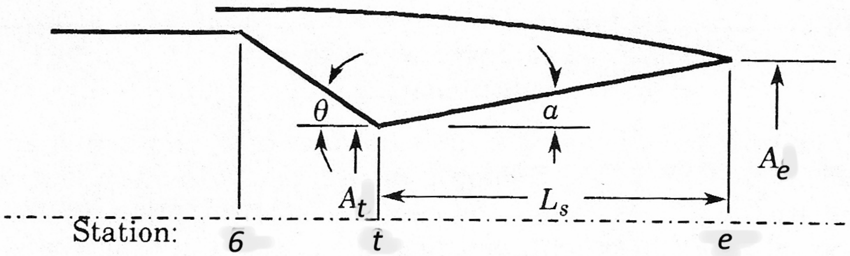

A_t - Primary nozzle throat area
A_e - Secondary nozzle exit area
α - Secondary nozzle half angle
θ - Primary nozzle half angle
L_s - Secondary nozzle length

Nozzle Geometric Parameters

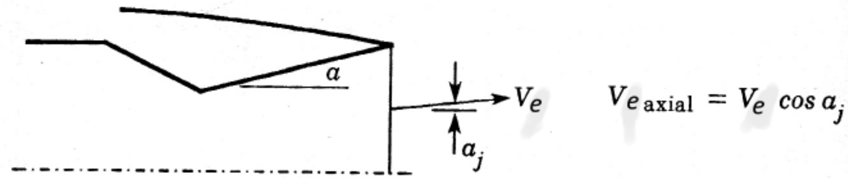

Local Angularity Coefficient

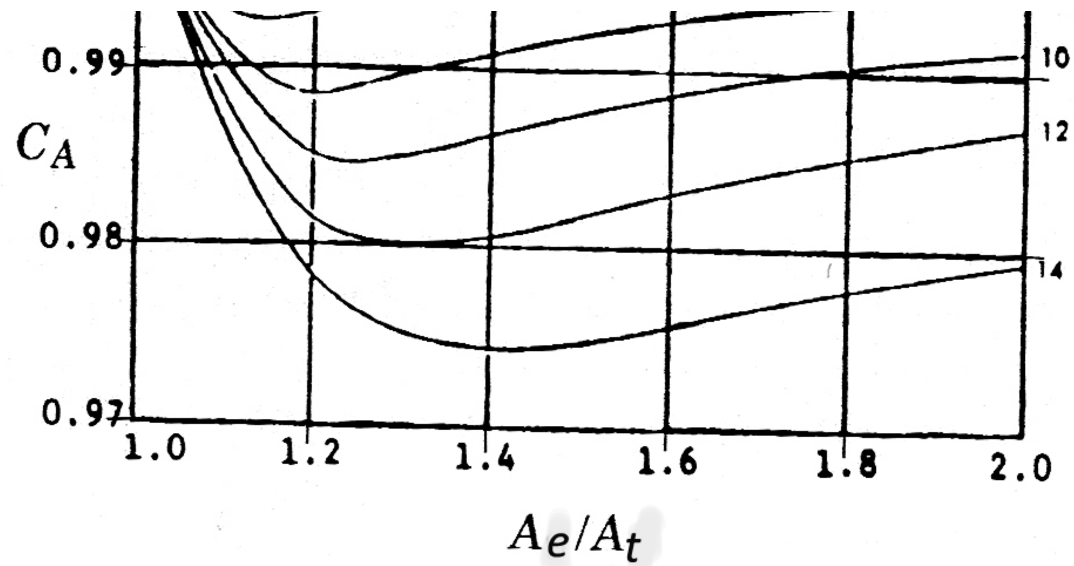

C-D Nozzle Angularity Coefficient

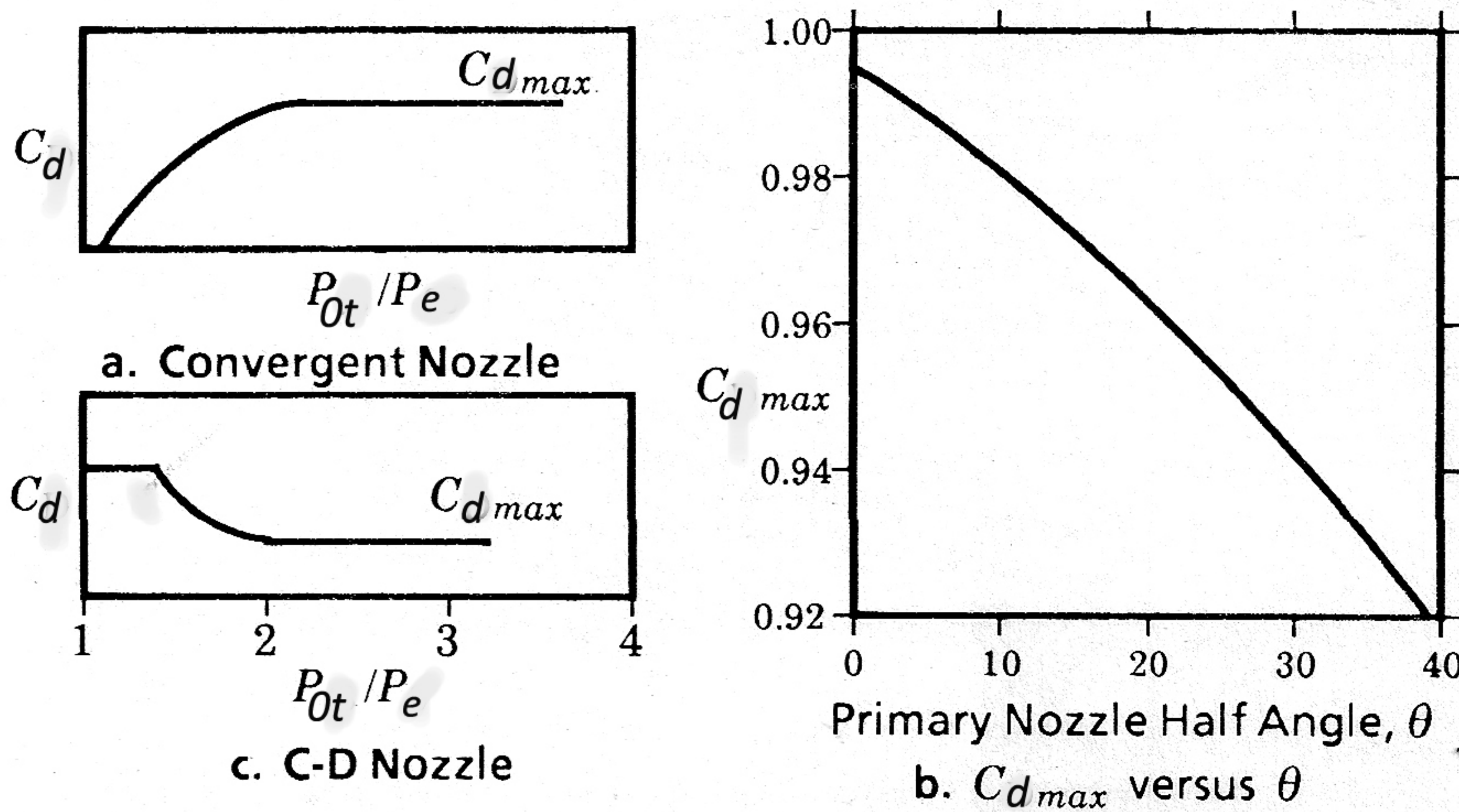

Nozzle Discharge Coefficient

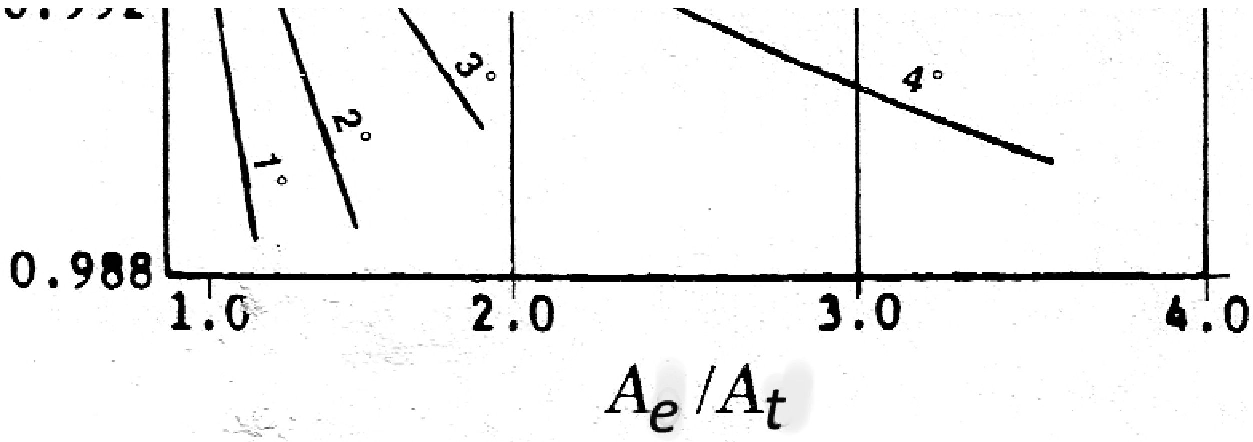

C-D Nozzle Velocity Coefficient